UNIVERSITY OF COPENHAGEN
DEPARTMENT OF MATHEMATICAL SCIENCES

Master's thesis

O-Lattice Interface Matching

Date: [15 August 2022]

Supervisor: Peter Krogstrup, Co supervisor: Tobias Særkjær

Institute:	University of Copenhagen
Author:	Sebastian Riis Reventlov Husted
Title and subtitle:	O-Lattice Interface Matching
Supervisor:	Peter Krogstrup
Co-supervisor:	Tobias Særkjær
Date:	15 08 2022

Table of content

1 Abstract

In this thesis we present a model which can identify which orientation of two crystals would form well matched interfaces. Based on geometric interface matching we are able to identify certain orientations which in the context of epitaxial growth may lead to the formation of stable interfaces with few grain boundary defects as result. Due the purely geometric approach the model, to model is unable to determine whenever the desired interface match would be allowed by the growth kinetics that governs the exchange of atoms between grains in the film. The model presented here is highly useful under circumstances where we have an empirically founded idea of which out of plane orientations to expect.

Danish:

I dette speciale præsentere vi en model der kan identificere hvilke orienteringer af to krysaller, der ville forme en god samenhængede grænseflade. Baseret på det geometriske grænseflade match er vi i stand til at identificere bestemte orienteringer, der i kontexten af epitaxiel krystalvækst, kunne lede til stabile grænseflader med få korngrænser som resultat. Siden modellen er baseret på rent geometriske betragtninger, er den ude af stand til at kunne konkludere hvorend det ønskede grænseflade match ville være tilladt af som konsekvens af vækstkinetik. Modellen præsenteret her er dog bemærkelsesværdig brugbar i de tilfælde hvor vi har en empirisk baseret idea af hvilke orienteringer vi kan forvente ud af planet af grænsefladen.

2 Introduction

The insights provided by the field of quantum mechanics has allowed for an unprecedented advancements in technology. Everyday devices such as the phone, GPS, and the computer this thesis was written on have been made possible by the passive exploitation of quantum effects. In recent times there has been a great interest in the advancement of quantum technology, as to create devices which can actively control quantum effects[1]. One such example is the quantum computer, which if realized would have the ability to solve problems classical computers are incapable of. A major challenge in the realization of large scale quantum computing comes from decoherence caused by interactions with the environment. As the advances in growth methods has enabled the manufacture of atomically abrupt heterointerfaces, the exotic physics that arises from a hybrid interface may provide a good platform for the formation of Qubits. As the hybrid interface in the heterostructure is atomically flat, a significant difference in lattice parameters may result in the build up of huge strains that would lead to the formation of defects as the thickness of the growing material increases[2]. For Qubits based on heterostructures, the formation of defects will cause significant scattering, which will in turn lead to decoherence[3]. In general, while certain materials may have electronic properties which would be beneficial for heterostructure devices that can actively harness quantum effects, when the materials are not commensurate this generally leads to defects which results in lower mobility and overall lower quality. Furthermore even for classical devices such as transistors, as the size of the devices shrink, the interfaces constitute an increasingly large part of the system[4].

In order to properly utilize the electronic properties of different materials, we have to choose combinations of materials for which the interfaces formed are largely stable and free of defects.

To attain stable and defect free hybrid interfaces, a purely geometrical approach may provide with a starting point. In this thesis we present a model which can calculate the interfacial match of between two crystal surfaces based on a geometric approach. The theoretical framework that underpins the model is based on the $O-Lattice\ theory$ [5]. Our use of this theory is to find coinciding lattice points of two interpenetrating lattices which represents the structure of two crystals. By freely rotating either lattice we may find certain orientations which maximize the density of coinciding lattice points within the interface plane, without needing to excessively strain either lattice. The interfacial match is quantified in terms of the density of coinciding lattice sites within the habit plane of the interface boundary, and the geometric strain needed in order to achieve the match. This provides information on how well an interface boundary matches, depending on the orientation of the crystals.

In relation to the growth a thin film a substrate, the grain boundaries defects which may appear will depend on the relative orientation between the grains in the film.
Therefore the grain boundaries that may occur between to grains which both have a good interfacial match with the substrate, can be determined based on the relative orientations of grains which can be inferred from the interface match with the substrate. The purpose of our model is then to find orientations of grains which would form a well matched interface with the substrate, and coherent grain boundaries(or even single crystals) between the grains composing the film. As such, we are trying to optimize the system as a whole.

Since the growth of thin film is dependent on energetics, and not geometry, the growth may not facilitate the growth of the desired grain orientation that the model predicts would lead to stable interfaces match we few or none grain boundary defects. In short, it may be that orientations of grains would lead to a higher quality device performance, but the energetics results in that another subpar(in terms of grain boundaries formed, and interface match) grain orientation would dominate the growth within the film. As the role of strain induced by the interfacial match, and the grain boundary defects that arises as result, within the context of grain growth, increases with larger film thicknesses. This might lead to new preferred grain orientations as the growth kinetics that governs the exchange of atoms between grains, would increasingly strive towards the elimination of highly strained grains and incoherent grain boundaries.

In order for a theoretical model to accurately determine the overall interface match between the film and the substrate and grain boundaries that would result from the growth of a thin film, the model would have to simulate the relevant growth kinetics that governs the growth of the thin film. Such a model is unfortunately outside the scope of this thesis, and may be the subject of future work. However, the model presented in this thesis allows us to gain insight in which orientations would lead to highly matched interfaces with little to no strain need to attain this match, as well as which grain boundaries may then form as a consequence of the interfacial match. As such, based on simple geometric considerations, the model serves as a starting point for identifying material combinations whose structural properties may lead to largely stable interfaces and with few or no grain boundary defects. Since the model relies on a purely geometrical approach, further theoretical and experimental studies is required in order to conclude if the growth would result in the desired interface match, and whenever or not, this match would translate into a higher quality device performance.

In order to put the interface matching in perspective with regards to the growth of a film of a crystalline solid, we give a brief outline on the subject matter at hand in the following sections. Here we present relevant theory from [6] as to attain insight, in how the grain boundaries, and the interfacial match with the substrate affect the evolution of the film.

In the case of the growth of Al on a hexagonal InAs nanowire, the model provided at highly coincident interface match between the $\{11\bar{2}\}$ surface of the Al, and the $\{1\bar{1}00\}$ side facets of the InAs nanowire. The interface match required the Al to orient the $\langle 111\rangle$ direction along the nanowire length, which resulted in two distinct structural variants of Al which obtains the same interface match. Due to difference in relative orientation, the Al grains on neighboring nanowire facet would either form twin boundaries or a single crystal depending on the structural variant of the grains(see figure 8). In the case of the growth of a layer of Pb on a hexagonal InAs nanowire the model provided the best interfacial match for the $\{11\bar{2}\}$ surface of Pb with the $\{1\bar{1}00\}$ side facets of the InAs nanowire. Due to the orientation of the $\{11\bar{2}\}$ surface on the InAs facet, the Pb grains on adjacent nanowire facets was unable to form coherent grain boundaries. On the other hand the $\{111\}$ surface of Pb was able to form a less coincident interface with the $\{1\bar{1}00\}$ side facet of the InAs nanowire. Due to the orientation of the $\{111\}$ plane, the Pb grains on neighbouring facets could form small wedge grain at the corner of the nanowire facets which formed a twin boundary and $\Sigma = 11$ boundary with the Pb grains surrounding the wedge grain at the cost of some strain for the wedge grain.

3 Growth of thin film

In this thesis we consider how the growth of a film of a crystalline solid on a substrate depends on the interfaces formed with the substrate and with the neighboring grains in the film.
In the case of growth done by the means of molecular beam epitaxy(MBE), the surface of the substrate is targeted by an incoming beam flux of atoms. These atoms from the beam may then adsorb onto the surface of the substrate as adatoms, which then diffuse across the surface of the substrate and then either desorb and effectively disappear from the system, or incorporate into a solid phase; material is grown.
As more and more adatoms incorporate into a solid phase, small islands are formed on the surface of the substrate. The density and morphology of these islands is a study in and of itself, but for our purposes we merely note that islands can nucleate and form separately and somewhat independent from one another.
As growth continues, the islands increase in size and density, eventually enveloping the surface of the substrate; islands coalescence has produced a thin film, and the former islands now make up grains in the film. Since the grains initially nucleated as separate islands, the solid phases may differ between grains.
The further evolution of these grains then comes in two varieties; the grains may grow in the direction normal to the substrate surface by incorporating additional atoms supplied by the incoming beam flux, or grains may change their lateral size by exchange of atoms between neighboring grains, causing grain boundary movement.

Ultimately, grain boundary movement is governed by the exchange of atoms between neighbouring grains. The exchange kinetics are governed by the chemical potentials associated with different grains, and evaluation of a grain type as a whole, as such lets us quantify part of the excess chemical potentials. In short, the evolution of the film is heavily influenced by how each grain in the film interacts with is local environment. In the following section we will present some of the theory and formalism from [6] to show how the growth kinetics for a grain depends on the environment.

3.0.1 Growth kinetics

This section follows the formalism from [6]. We wish to quantify the growth in terms of thermodynamic parameters, and since the growth of the crystal is a process that occurs far from a thermodynamic equilibrium, we may therefore find it convenient to refer to an equilibrium reference state(ERS). In this formalism a phase may find it self in a local state

p, where p takes on the mean intrinsic properties of its local environment. The size of local environment is such that the local state p is able to represent thermodynamic properties its immediate surrounding.In Addition the local environment that defines the properties of p, is only defined within main state p resides in. If p refers to a local state within a grain in a thin film, the local environment that defines p is confined within the grain the local state p resides, such that p represents only the thermodynamics properties of that grain. The excess chemical potential of a phase in the state p with respect to the ERS is then given as.

$$\delta\mu_{p-ERS} = \mu_p - \mu^{ERS} \tag{1}$$

Where μ_p is the chemical potential for a phase in the state p, and μ^{ERS} is the chemical potential of the ERS.

For a transition from a phase a the state p to another local state q, we have to reach a transition state (TS) before we may do so. The average rate of this transition will depend exponentially with the Gibbs free energy of activation associated with reaching the transition state. We may write the activation energy for reaching the transition state as:

$$\delta g_{pq}^{TS} = \delta g_{pq}^{TS,ERS} - \delta\mu_{p-ERS} \tag{2}$$

With $\delta g_{pq}^{TS,ERS}$ being the activation energy for a transition from p to q and $\delta\mu_{p-ERS}$ is the chemical potential at state p with respect to the ERS. In figure 1, the energy landscape of pq transition is shown.

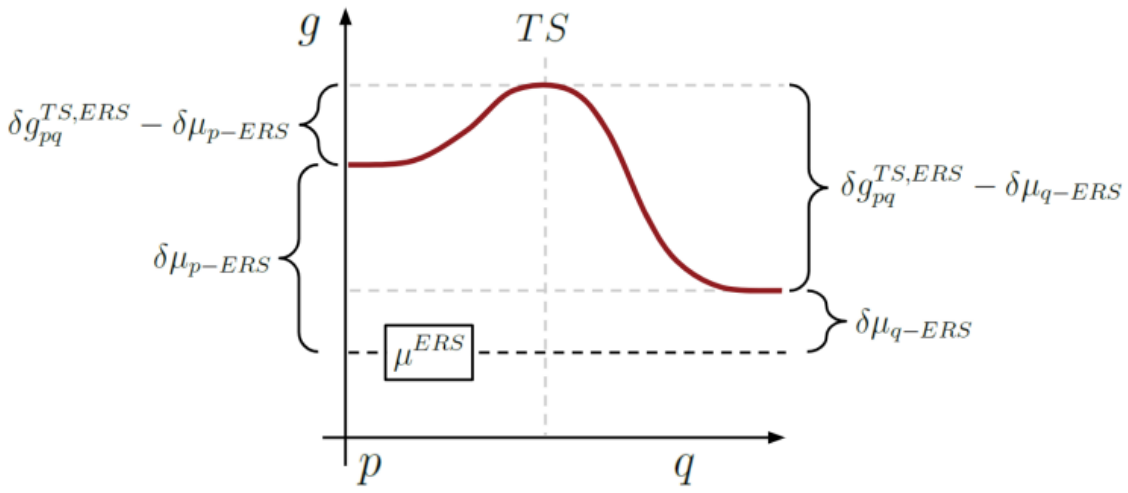

Figure 1: Energy landscape of transition: Adapted from [7]

The average transition rates of a flux of atoms per area, in the local state of p crossing

over the boundary of pq is given by:

$$\Gamma_{pq} = \begin{cases} \Xi_{pq} c_p exp(\frac{\delta g_{pq}^{TS,ERS} - \delta\mu_{p-ERS}}{k_b T}) \\ if \quad \delta g_{pq}^{TS,ERS} \geq \delta\mu_{p-ERS} \\ \Xi_{pq} c_p \\ if \quad \delta g_{pq}^{TS,ERS} < \delta\mu_{p-ERS} \end{cases} \tag{3}$$

Where Γ_{pq} is a single atom flux prefactor that accounts for the number of attempts for an atom does before it succeeds to pass from the state p to the transition state, while c_p is the concentration of atoms in the state of p.

If we further more apply that at ERS conditions the net flux across a the pq is zero, and we assume limited barrier kinetics, meaning that the activation energy required for reaching the transition state from the state p is larger than or equal to the chemical potential of the state p, we may write that the net flux from the transition from p to q as:

$$\Delta\Gamma_{pq} = \Xi_{pq} exp\left(\frac{-\delta g_{pq}^{TS,ERS}}{k_b T}\right)(c_p exp(\frac{\delta\mu_{p-ERS}}{k_b T}) - \frac{c_p^{ERS}}{c_q^{ERS}} c_q exp(\frac{\delta\mu_{q-ERS}}{k_b T})) \tag{4}$$

In the case of transitions between neighbouring grains we may set the concentration to either zero or an constant depending on when the grain in question occupies the space at p, which case the equations reduce to:

$$\Delta\Gamma_{pq} = \Xi_{pq} c_p exp\left(\frac{-\delta g_{pq}^{TS,ERS}}{k_b T}\right)\left(exp(\frac{\delta\mu_{p-ERS}}{k_b T}) - exp(\frac{\delta\mu_{q-ERS}}{k_b T})\right) \tag{5}$$

Since the sign of equation 5 depends only on $\left(exp(\frac{\delta\mu_{p-ERS}}{k_b T}) - exp(\frac{\delta\mu_{q-ERS}}{k_b T})\right)$, a netflux from a solid state p to another solid q would be positive if $\delta\mu_{p-ERS} > \delta\mu_{q-ERS}$, meaning that a the grain at q will grow at the expense of the grain at p, and vice versa. Therefore only $\delta\mu_{p-ERS}$ and $\delta\mu_{q-ERS}$ determines the which grains will grow and which grains will shrink. The excess chemical potential for local solid state with respect to the ERS is given as:

$$\delta\mu_{s-ERS}^{X} = \sum_n \gamma_n \frac{\partial A_n}{\partial X}\frac{\partial X}{\partial n_p} + \Delta\epsilon_s \tag{6}$$

Where $\delta\mu_{s-ERS}^{X}$ is the change in excess Gibbs free energy per atom for solid with respect to a change of parameter X which defines the shape of the solid. γ_n is the excess surface free energy of the n'th interface, A_n is the area of that interface, while n_p is the number of atoms in the state of p. The final term $\Delta\epsilon_s$ is a contribution from the strain for a change in X.

The $\frac{\partial A_n}{\partial X}$ tells that the contribution to the excess chemical potential from the n'th interface increases if the area of n'th interface increases as a result of a change in the shape parameter X. If the change in X would reduce the area of an interface, the contribution to the chemical potential from that interface would therefore reduce the chemical potential.
From $\frac{\partial X}{\partial n_p}$ the contribution to the chemical potential scales inversely with the number of atoms needed to cause a change in the shape parameter X. Such that if an increase in X would result in large increase of atoms in the grain, the contribution to the chemical potential is lower than if, an increase in X would result in relatively lower increase in atoms of the grain.
The final term $\Delta\epsilon_s$ results from strain induced in the crystal structure of the grain, which takes into account the excess energy needed to move an atom into the strained structure of the grain. As such if a change in the shape parameter X would increase the number of atoms in a strained grain, the contribution to the chemical potential would likewise increase.

The first term in equation 6 is a sum of contributions from the interfaces of a solid, which for a grain in a thin film the relevant interfaces can be grouped into three sets. The first set of interfaces, are the interfaces between the grains with vacuum with excess surface free energy denoted $\gamma_{S,n}$ for the n'th interface between the grain and vacuum.
The second set of interfaces are the interfaces between the grain and the surface of the substrate with the interface energy density $\gamma_{I,n}$ for the n'th interface between the grain with the substrate surface.
The third set of interfaces are the interfaces between the grain and the neighbouring grains in the thin film with the interface energy density denoted $\gamma_{GB,n}$ for the n'th grain boundary interface.
From now on, the interfaces of the grain with vacuum are referred to as the top surfaces of the grain, the interfaces between grains as the grain boundaries, and the interface between the grain and substrate surface as the substrate interface.
In figure 2 a sketch of a thin film on substrate with the relevant interfaces and their interfacial energy densities shown.

$$\delta\mu^X_{s-ERS} = \sum_{S,n} \gamma_{S,n} \frac{\partial A_{S,n}}{\partial X} \frac{\partial X}{\partial n_p} + \sum_{I,n} \gamma_{I,n} \frac{\partial A_{I,n}}{\partial X} \frac{\partial X}{\partial n_p} + \sum_{GB,n} \gamma_{GB,n} \frac{\partial A_{GB,n}}{\partial X} \frac{\partial X}{\partial n_p} + \Delta\epsilon_s \qquad (7)$$

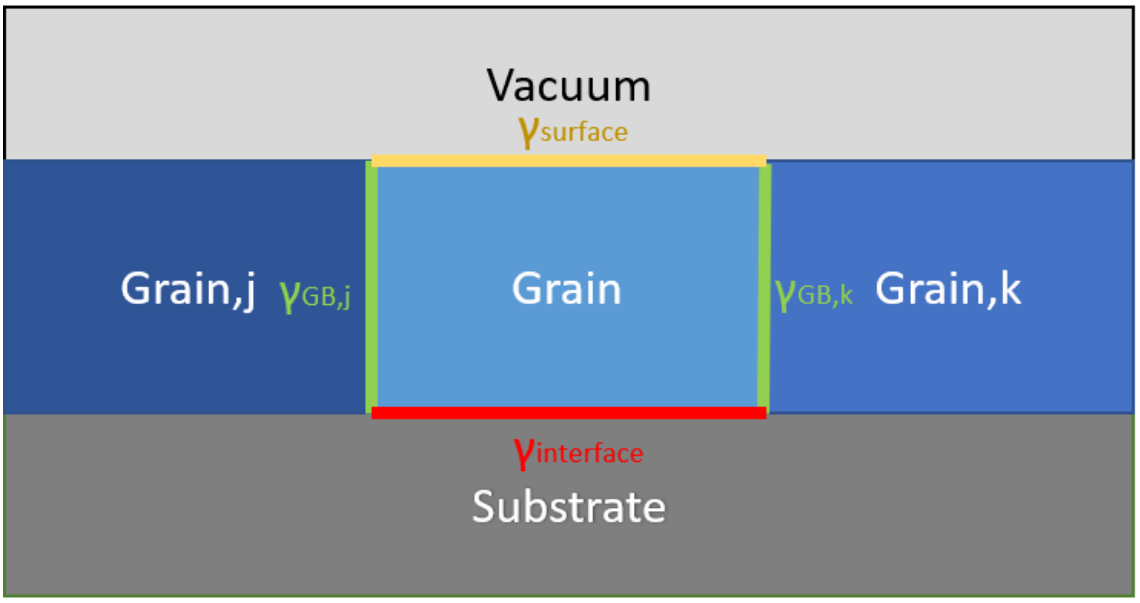

Figure 2: Grain in a thin film: In blue grains composing the thin film with different shades of blue to denote different phases. In dark grey the substrate. In light grey vacuum. The green lines refers to grain boundaries formed due a difference in orientation between the neighbouring grains with $\gamma_{GB,n}$. The red line refers to the substrate interface between the grain and substrate with $\gamma_{I,n}$. The yellow lines refers to the top surface of the grain with $\gamma_{S,n}$.

We will now very superficially consider the effect of the chemical potential will have on the growth of a thin film on a planar substrate.

As mentioned the contribution to the excess chemical potential scales from an interface scales with the increase in area as a result of an increase with regards to a shape parameter X.
For an exchange of atoms between grains which results in growth of a grain along the plane of the substrate surface, the contributions to the chemical potential from the top surface of the grain and the contribution from the substrate interface scales with the resulting increase in area of top surfaces and substrate interface respectively.
On the other hand the contributions from the grain boundaries will scale with the resulting increase in area of the grain boundary i.e scale with the thickness of the film. Finally the contribution from the strain will increase with the overall volume of the grain.
Since the area of the grain boundary depends on the thickness of the film, the contribution to the chemical potential from the grain boundaries will be negligible compared contributions from the top surface and substrate interface while the thickness of the film is small compared to the width of the grains.

For the atoms that belongs to the top surfaces of the grains, there will always be some

dangling bonds, while for the atoms at the substrate interface between the grain and the substrate this may not be the case. Depending on the orientation and crystal structure of the substrate, some of the atoms of grain at the substrate interface may form bonds with those of the substrate thereby reducing the number of dangling bonds. For a top surface(or substrate interface), with a high density of dangling bonds, should roughly translate into a high top surface(or substrate interface) energy density, and vice versa.

While these considerations are nowhere near the complete description of the surface and interface energies, the overall picture should still be approximately correct. As such we would expect that the top surfaces of the grains would contribute more to the chemical potential than the contribution from the substrate interface. In addition the interfacial match between an grain with a fixed orientation normal to the substrate surface, and the substrate may have a lower number of dangling bonds for certain orientations in the plane of the substrate surface. As such the contribution to chemical potential will depend on the orientation of grain in the plane of substrate surface.

The orientation of the grain normal to substrate interface is denoted as the out of plane orientation of grain, where the plane in question refers to the plane of the grain at the substrate interface. Likewise the orientation of the grain at the substrate interface is then denoted as the in plane orientation of the grain, i.e. changing the in plane orientation refers to rotation around the interface normal.

To reiterate from earlier, the dominant contributions to the chemical potential associated with the in plane growth of a grain, are those from the contributions from the top surface, and the substrate interface.
The contribution from the top surface depends only on the out of plane orientation of the grain, while the contribution from the substrate interface depends on both the out of plane orientation and the in plane orientation of the grain.

Per our discussions, leading up to and including equation 5, grains with an out of plane orientation and in plane orientation that minimizes the overall contribution from the top surfaces and substrate interface, would therefore grow at the expense of other grains with an orientation that does not minimize these contributions.
In this regime where the thickness of the film is negligible compared to the width of the grains, the overall growth kinetics are dominated by the surface excess chemical potential contributions from the top surface and the substrate interface.

As mentioned earlier the contribution from the top surface is generally larger than that of the substrate interface. Thus it may often be the case that the preferred out of plane orientation (the out of plane orientation which minimizes the contribution to the chemical potential from the top surfaces and substrate interface) would be the out of plane orientation minimizes the contribution from the top surfaces. In this case the preferred in plane orientations of a grain, would be the in plane orientations which minimizes the contribution from the substrate interface.
It may very well be the case that a out of plane orientation of grain would minimize the contribution from the top surfaces, but the interfacial match with the substrate surface for that particular out of plane orientation would lead to an overall larger contribution to the chemical potential, compared to another out of plane orientation of the grain that may form a better interfacial match which in turn would minimize the overall contributions to the chemical potential from the top surfaces and substrate interfaces.
As such the preferred out of plane orientation and in plane orientations of the grains, depends on the interfacial match at the substrate interface, as well as the excess surface free energy of the top surfaces.

For a fixed out of plane orientation there may be several in plane orientations which produce the same interfacial match, and depending on the symmetry of the bulk structure of the grains and the symmetry of the substrate interface, there may be a degeneracy in preferred orientations of the grains.
These degenerate orientations leads to different phases of the grains which should be equally favoured by the in plane growth, and would therefore lead to the formation of grain boundaries between grains of different phases. Furthermore, in order to achieve a good interfacial match, and therefore reduce the contribution from the substrate surface, it may be necessary to induce strain into the crystal structure of the grain (strain induced into the substrate can be thought of as an additional strain cost for the grain).

As the thickness of the thin film increases area of the grain boundaries also increases, and the increased size of the grains would likewise result in an increase in the contribution from the grain boundaries as well as the induced strain. As such the contributions from these two factors would become increasingly important in regards to the in plane growth a grain as the thickness of the thin film increases.
The in plane growth of a grain would lead to an increase in the area of the top surface and substrate interface that is largely independent of the thickness of the film. Therefore the

contributions from the top surface and the substrate interface will be decreasingly important to the driving force for in plane growth, relative to the contributions the grain boundaries and strain at larger film thicknesses. Thus, at some film thickness the growth enters a regime where the grain boundaries and the strain are the dominant contributions to the driving force of in plane growth.

If the in plane growth would result in an increase of the area of grain boundary with a high grain boundary energy, it would result in a higher contribution to the chemical potential. Therefore the in plane growth of a grain would facilitate the movement of grain boundaries, as to eliminate grain boundaries with a high interface energy density. It may be that new out of plane orientation and corresponding in plane orientations which would reduce the contributions from the grain boundaries and the induced strain. As such incoherent grain boundaries and the strain induced from interfacial match with the substrate, may provide the necessary conditions to facilitate a reconstruction into grains with an out of plane orientation and in plane orientation which would significantly reduce these contributions.

Depending on the height of the islands at the point which they coalescence into a film, the grain may never enter the regime where the top surfaces and substrate interface are the dominant driving force for in plane growth. In such a case, upon formation of the film, the in plane growth is governed by the contributions from the grain boundaries and the strain induced by the interface matching.

Predicting which choice of materials and crystal orientations will lead to stable interfaces between the entire thin film and a substrate is difficult, and a extensive model of the growth behavior that could conclude which material combination would form stable interfaces is out of the scope of this thesis.

While the contribution to the chemical potential from the top surfaces of grain is independent of the interfacial match between the grain and the surface of the substrate, the contributions to the chemical potential from the substrate surface, the grain boundaries, and the contribution from the strain depends with varying degrees on the interfacial match. Obliviously the contribution from the substrate surface to the chemical potential associated with the in plane growth of grain, depends very directly on the interfacial match. The same is of course true for the strain induced in the crystal structure of the grain in order to achieve the interfacial match.

The contribution from the grain boundaries does to a degree also depend on the interfacial match, since the grain boundaries depends on the relative orientation between two grains, and the location of the grain boundary plane. As the in plane orientation of a grain depends on the interfacial match, thus the relative orientation between two grains also depends to some degree on interfacial match.

In this thesis we present a model which can evaluate the interfacial match between a grain with the substrate surface. The evalutation of interfacial match is quantified by two parameters: Firstly, the area of the coincidence site lattice formed between the lattice planes of the grain and substrate at the substrate interface.
Secondly, the geometric strain of crystal lattice of the grain (or substrate) needed to form a coincidence site lattice at the substrate interface.

The area of coincidence site lattice is measure of the density atoms in the habit plane of the substrate interface, which fits into the crystal structure of both the grain and substrate. Since a higher density of atoms that fits in both crystal structures, would correspond to a lower density of dangling bonds at the substrate interface, the interface energy density of the substrate interface γ_S is therefore related to the area of the coincidence site lattice.
While γ_S depends on material parameters, the area of coincidence site lattice is a purely geometric parameter. While the exact relation between γ_S and the area of the coincidence site lattice is unclear, an increase in the area of the coincidence site lattice should correspond to an increase in γ_S. Therefore while the value of γ_S may be unknown, the geometric approach would enable us to find which in plane orientation of a grain results in minimum of γ_S.

While these two geometric parameters alone does not provide the direct values of γ_S and $\delta\epsilon_s$, the area of the coincidence site lattice should provide which in plane orientation of a grain we would find a minimum in γ_S, and the geometric strain should yield a minimum in $\Delta\epsilon_s$ when no geometric strain is needed to form a coincidence site lattice.
In the following sections we present relevant theory behind the coincidence site lattice, and use that to make model which will allow us to evaluate the interfacial match.

4 Interface matching

As mentioned earlier, the theoretical framework behind the model is based on the O-lattice theory from [5]. In the following section the will give introduction to key concepts behind O-lattice theory and how we may apply that O-lattice theory to find well matched interfaces.

4.1 Coincidence site lattice theory

In order to grasp how an arbitrary interface between two layers of crystalline solids depends on the crystal orientation of the solids, we will start by presenting a brief overview of the coincidence site lattice theory. Initially we will consider how we can describe grain boundaries using the relatively simple coincidence site lattice theory, and later on show how the more complicated O-theory can be used to describe more general interfaces between two solids.

As mentioned above we will first deal with grain boundaries between two crystalline solids of the same material, which are defects that occurs due to difference in orientation between the two grains. At the contact interface of the two grains, we have the plane of our grain boundary which it self also have some orientation with respect to the grains.
Depending on the orientation of two grains relative to each other as well as the orientation and location of the boundary plane between the two grains, there may exists lattice sites of both grains at the boundary plane which physically coincide on both crystal lattices. We dub these lattice points as a "coincidence lattice site".

For an atom located at such a site, would perfectly fit in the crystal structure of both grains, and is therefore no need to adjust the bond length or induce strain in the crystal structure for the grains. These coinciding lattice sites therefore as well reduce the number of dangling bonds of both crystals, as the bonds to the coinciding lattice site with the atoms from on both sites of the boundary matches to the crystal structure of both grains.

Therefore a grain boundary plane which would contain a high density of these atoms located at a coinciding site, would yield a better interfacial match for the boundary as the boundary plane would contain a higher density of atoms which lowers the amount of dangling bonds of both crystals, which in turn would yield a lower grain boundary energy.
Conversely for a grain boundary with a low density of coinciding lattice sites, the amount of dangling bonds increase, and furthermore we may have to induce strain in the crystal lattices in order to fit the position of atoms and thereby achieve a interfacial match.
This would result in that the grain boundary energy would be a lot higher, and we may have

to introduce certain defects such as dislocations in the crystal in order to achieve a stable boundary.

We may always find at least one coinciding lattice site by doing a translation of the crystal lattice of one grain, such that we move a lattice site corresponding to an atom of one grain on top of an arbitrary lattice site of the second grain. The idea is then to find orientations of one grain relative to the other grain for which we may produce an infinite amount of coinciding lattice sites. These infinite coinciding lattice sites is formed by the "coinciding site lattice".
The coincidence site lattice, is as the name suggest a lattice formed by the coinciding sites of both grains of the boundary. Simply put, if we where to take two neighbouring grains and continue the crystal lattice of both grains into their respective neighbour grain we might see that at some point, that the there is a coincidence of atoms for the interpenetrating lattices.

The lattice that connects these coinciding atoms, is then the coincidence site lattice. Since it is generated by coinciding atoms of belonging to either crystal, the Coincidence Site lattice can be reached translation vectors belonging to both crystal lattices, therefore the coincidence site lattice belongs to both crystals. The lattices vectors of the coinciding site lattice are then the translation vectors of either crystal lattice of the grains which reach an coinciding lattice site.

The volume of the coincidence site lattice unit cell in units of the unit cell of the generating lattice, is written as $\Sigma = n$, where n is an integer. This is our first measure of what might might be a good orientation relationship between boundaries.

For a low sigma value, such as sigma = 3 it means that every third elementary unit cell of the crystal lattice would contain coinciding sites i.e every third atom would be an atom in both crystals, and for sigma = 1 we every atom would be coincident. We might be tempted to think that a low Sigma value naturally would be a better boundary due to a higher concentration of coinciding atoms compared to higher values of sigma, we do not have the entire picture as we have neglected to consider the orientation of the boundary plane.

Depending on where we make our boundary plane we get very different results. If the boundary plane contains sites that corresponds to atoms of only one of the crystals, the atoms of the boundary will need to adjust in order to fit the boundary to the other crystal. The structure of such a boundary would in general by less energetically favourable, compared

to a boundary consisting of only coincident lattice sites, for reasons we mentioned earlier. The optimum boundary plane would therefore be the plane that intersects as many coincident sites as possible, from which we can infer that boundaries that contains a coincidence site lattice which yields low sigma value are preferable since a smaller unit cell of the CSL means that the coincident sites are closer packaged together.

4.1.1 Example: CSL of a 2D square lattice

As an example we consider an interface of two square lattices, A and B. For any lattice we may center the origin at an atomic site, such that for both square lattices the origin contain an coinciding lattice site. The rest of the atomic sites can then be found by doing translations from the origin by combinations of the base translation vectors of the lattices. This way we ensure that if we find two vectors from the origin that reaches a coinciding lattice site, these two vectors would produce a coincidence site lattice.
For a 2 dimensional lattice, the base translation vectors in the basis of the lattice coordinate system are $\vec{t_1} = \binom{1}{0}$, and $\vec{t_2} = \binom{0}{1}$.
For the square lattice A, we consider in this example $\vec{t_1}$ is aligned along the x-axis in real space, while $\vec{t_2}$ is aligned along the y-axis in real space, both being of equal length. For the square lattice B, the base translation vectors would be of equal length with a 90° angle between them, but alignment in real space would depend on the relative orientation between lattice A, and lattice B.
In this case the coincidence site lattice must also be square lattice, since for each point rotated over the x-axis, a similar point must be rotated over the y-axis. For a vector of lattice A which points to a coinciding site (x, y), there must exist a corresponding vector pointing to coinciding lattice which is orthogonal to vector that reaches the point (x, y) with the same length. The surface spanned of these vectors is then given by:

$$\Sigma' = |x|^2 + |y|^2 \tag{8}$$

It should be evident that x and y should contain common factors, as this would mean that a fraction of these coordinates also contains an coincident site. If $\Sigma' = n$ where n is an even number, which would require that both x, and y to be an uneven number, then it should be possible to form a coincidence site lattice which half as big, $\Sigma = \Sigma'/2$. The sum of vectors that spans the unit cell of the coincidence site lattice $(x, y) + (-y, x) = (x - y, x + y)$ in the case of x and y are uneven, it would mean that $(x - y, x + y)$ would be an even number,

therefore an fraction of that vector would also reach a coinciding lattice site. In the case the lowest common divisor of $x-y, x+y$ is 2, Σ would then be given as:

$$\Sigma = |\frac{x-y}{2}|^2 + |\frac{x+y}{2}|^2 = \frac{x^2+y^2-xy}{4} + \frac{x^2+y^2+xy}{4} = \frac{x^2}{2} + \frac{y^2}{2} = \frac{\Sigma'}{2} \tag{9}$$

As such if Σ' is even then, we may always find another coincidence site point at the center of the square spanned by (x, y). Therefore for the coincidence site lattice, the unit cell area is always an odd integer. In the this case the rotation angle that produce the coincidence a value of Σ, can be found by:

$$\theta = 2arctan(y/x) \tag{10}$$

4.2 O-Lattice theory

The Coincidence site lattice model allowed one to grasp why some orientation relationship would lead to special grain boundaries, but beyond that the model is severely lacking. A reason for this, is that the coincidence site lattice is not physically meaningful, the grain-boundary structure that results from the coincidence site lattice, is physically meaningful however. This is due to the resulting grain-boundary contains coincident atomic sites, and is periodic with a periodicity which is given by the coincidence site lattice.

Since we only look for coincident sites, there might be other periodic grain-boundary structures for which there are no discernible coincidence site lattice. For two solids with different lattice constants, there is no guarantee that there even is a possible coincidence site lattice. Even for solids for the same material, if there is a different concentration of impurities in the solids the lattice constant will be slightly different, and there might not be a coincidence site lattice for any orientation.

If we were to make an infinitesimal change in the orientation relationship of the crystals that are in an coincidence site lattice configuration, we would expect an infinitesimal small change in the physical properties of the grain boundary. In the framework of the Coincidence site lattice model this would result in the loss of the perfect mathematical coincidence, and the situation have completely changed.
The problem for the coincidence site lattice model is its discreteness. In order to deal with any variation in crystal orientation, and lattice structure, we need a theory that is continuous. There is such a theory, namely the O-lattice theory, and in the following segment we will present the outline of the O-lattice theory.

If we have a lattice A, representing the crystal structure of one of the solids that constitute our grain-boundary, which after applying a transformation M, we end up in the lattice B, representing the crystal structure of other solid of the boundary. This transformation M can be anything as simple as a rotation around an axis for lattice of the same material, or it can be some other more complicated transformation that changes the lattice structure. More on the choice of M later, but for now simply note that M is the transformation that relates the crystal structure of A to the crystal structure of B.

If we have vector $\vec{r_A}$ that goes from the origin of lattice A to some point in lattice A, which will after the transformation M, point from the origin of lattice B, to some point in lattice B as the vector $\vec{r_B}$. These two points are said to be equivalent, since they have the same coordinates but in different basis.

$$\vec{r_B} = \mathrm{M}\vec{r_A} \tag{11}$$

Just to be clear, the equivalent points does not need to correspond to any atomic site on either lattice, they can be any where on the lattice.
For each equivalence points there is an infinite set of equivalence point, C_N, defined as the set containing the original equivalence point plus every point reachable by a lattice translation vector t_n from that point. Such that an point reached by $\vec{r_A}$ we may find an infinite set of equivalence points by:

$$\vec{r'}(C_A) = \vec{r}(C_A) + \vec{t_A} \tag{12}$$

Here $\vec{r}(C_A)$ refers to vector pointing to an equivalence point belonging to the set of points C_A, and $\vec{r'}(C_A)$ is the vector pointing to a another element in C_A found by doing a translation t_A of the lattice A.

The idea behind O-lattice theory is then to look for equivalent points, which are also coinciding.
An equivalence point is also coinciding if, the point in lattice A can reach its equivalence point of lattice B, by either performing the transformation M which marked the points as being equivalence points to each other, or doing translations belonging to those of lattice A.

$$\vec{r}(C_B) = \mathrm{M}\vec{r}(C_A) = \vec{r}(C_A) + \vec{t_A} \tag{13}$$

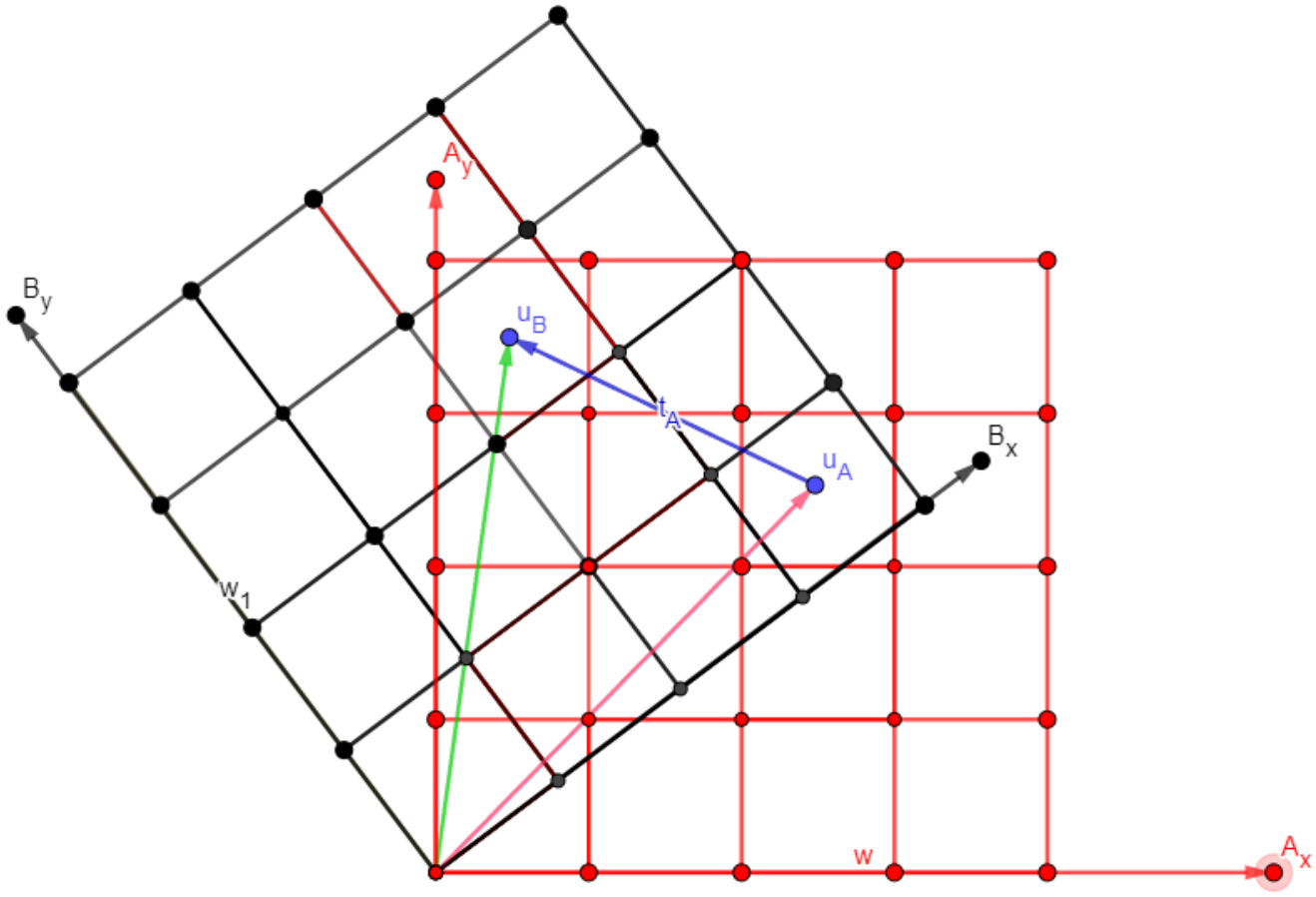

Figure 3: Two lattices; Lattice A(Red), which after a rotation yields lattice B(Black) The vector u_A then after the rotation that produces lattice B, yield the equivalent vector U_B. As a translation vector of A, t_A can reach U_B from U_A these points must be coinciding equivalence points

Since the point $\vec{r}(C_A)$ can reach its equivalence point $\vec{r}(C_B)$ of the lattice B, by means of transformation M or by the translation $\vec{t_A}$, then there is an element of the set of equivalence points of C_A which coincides with point reached by $\vec{r_B}$. In the same vein, there is also an element of C_B which coincides with the point reached by $\vec{r_A}$.

This means that while a point $\vec{r_A}$ in lattice A might not coincide with its equivalence point of lattice B $\vec{r_B}$, there is however a point in the set C_A which does coincide with the points in the set C_B.

We call these coinciding equivalence points for O-points and the vector $\vec{r}(C_O)$ is the vector that reaches an O-point of set C_O, which is the set of points that belongs to both C_A and C_B simultaneously.

$$\vec{r}(C_B) = \vec{r}(C_A) + \vec{t_A} = \vec{r}(C_O) \tag{14}$$

By utilizing that $\vec{r}(C_A) = \mathrm{M}^{-1}\vec{r}(C_B)$, we can write the following equation.

$$\vec{r}(C_O) = \mathrm{M}^{-1}\vec{r}(C_O) + \vec{t_A} \tag{15}$$

Which using the identity operator $\mathbb{I}$, we can rearrange into:

$$\vec{t_A} = (\mathbb{I} - \mathrm{M}^{-1})\vec{r}(C_O) = \mathbb{T}\vec{r}(C_O) \tag{16}$$

Where:

$$\mathbb{T} = (\mathbb{I} - \mathrm{M}^{-1}) \tag{17}$$

This equation 16 is known as the fundamental equation of O-lattice theory, and the solution of to this defines all the possible O-points of the lattices.
To reiterate, the solution to this equation will be the coinciding equivalence points or O-points of the lattices, so if a point in the center of a unit cell in lattice A is a solution, its equivalence point of lattice B will be located in the center of a unit cell in lattice B, and the two points will perfectly coincide in the real space coordinates. To solve for the O-points we simply invert the matrix to find the following:

$$\vec{r}(C_O) = (\mathbb{I} - \mathrm{M}^{-1})^{-1}\vec{t_A} \tag{18}$$

Provided that $|\mathbb{I} - \mathrm{M}^{-1}| \neq 0$. The O-points we find using this equation will form the O-lattice, which will be discussed at length later on. For now we will show an example of how to calculate the O-lattice, from a relatively simple situation.

4.2.1 Example: O-lattice of 2D square lattice

In this example we consider two 2-dimensional square lattices related by a simple rotation,i.e the lattice constants of both lattices are the same. The transformation operator is then given by a pure rotation matrix:

$$\mathrm{M} = \mathrm{R} = \begin{bmatrix} \cos\theta & -\sin\theta \\ \sin\theta & \cos\theta \end{bmatrix} \tag{19}$$

Which by inversion turns into following:

$$\mathrm{M}^{-1} = \begin{bmatrix} \cos\theta & \sin\theta \\ -\sin\theta & \cos\theta \end{bmatrix} \tag{20}$$

Inserting this into our equation (17) yields:

$$(\mathbb{I} - \mathrm{M}^{-1}) = \begin{bmatrix} 1-\cos\theta & -\sin\theta \\ \sin\theta & 1-\cos\theta \end{bmatrix} \tag{21}$$

The determinant has to be non zero for there to be a solution, and therefore an O-lattice, and in our example we find $|\mathbb{I} - \mathrm{M}^{-1}| = 2(1-\cos\theta)$, which is zero in the case of $\theta = n\pi, n = 0, 1, 2, ..$ where there is no structural difference in the two lattices. By matrix inversion we find the following:

$$(\mathbb{I} - \mathrm{M}^{-1})^{-1} = \begin{bmatrix} \frac{1}{2} & -\frac{cotan(\theta/2)}{2} \\ \frac{cotan(\theta/2)}{2} & \frac{1}{2} \end{bmatrix} \tag{22}$$

For a square lattice, the basic translations vectors of lattice A are $\vec{t_{A,1}} = \binom{1}{0}$ and $\vec{t_{A,2}} = \binom{0}{1}$. As such the basis vectors of the O-lattice are the column vectors of the matrix, which is trivial to see.

$$\vec{u_{O,1}} = \begin{pmatrix} \frac{1}{2} \\ \frac{cotan(\theta/2)}{2} \end{pmatrix}, \vec{u_{O,2}} = \begin{pmatrix} -\frac{cotan(\theta/2)}{2} \\ \frac{1}{2} \end{pmatrix} \tag{23}$$

These are then the base vectors of the O-lattice.

Unlike the coincidence site lattice, for which a change in the rotation angle would lead to its disappearance, the O-lattice vectors found undergoes smooth transitions in regards to a change in the rotation angle.

The relation between coincidence site lattice, and the O-lattice should become clear in the case where $cotan(\theta/2) = 3$, which happens near $\theta \approx 36.87°$. The O-lattice vectors then yields:

$$\vec{u_{O,1}}(\theta \approx 36.87°) = \begin{pmatrix} \frac{1}{2} \\ \frac{3}{2} \end{pmatrix}, \vec{u_{O,2}}(\theta \approx 36.87°) = \begin{pmatrix} -\frac{3}{2} \\ \frac{1}{2} \end{pmatrix} \tag{24}$$

Here it should be noted that $\begin{pmatrix} \frac{1}{2} \\ \frac{3}{2} \end{pmatrix}$ and $\begin{pmatrix} -\frac{3}{2} \\ \frac{1}{2} \end{pmatrix}$ does not refer to an atomic position within either lattice, since only O-points that can be expressed as integer combinations of the base vectors of lattice A, refers to an atomic site.

However, since the denominator of the O-lattice base vectors is 2, then every second O-point would be an integer combination of base vectors of lattice A, i.e every second O-point refers to an atomic site in both lattices. These O-points refers to atoms in both lattices A, and B, which coincide with each other, as such the lattice found by connecting these O-points will be the coincidence site lattice of this configuration.

Therefore one may find a lattice of O-points which are also atomic sites by:

$$2 \cdot \vec{u_{O,1}} = \begin{pmatrix} 1 \\ 3 \end{pmatrix}, 2 \cdot \vec{u_{O,2}} = \begin{pmatrix} -3 \\ 1 \end{pmatrix} \tag{25}$$

Where the volume of the unit cell of this lattice, in the units of unit cell of lattice A, would be simply $\frac{\sqrt{1^2+3^2}\cdot\sqrt{(-3)^2+1^2}}{1} = \frac{3^2+1^2}{1} = 10$. This means that the O-lattice found, would correspond to a $\Sigma 10$ boundary configuration in the coincidence site lattice terminology. While a lattice of coinciding lattice sites was found by these O-lattice vectors, this lattice does not contain every coinciding lattice site. For this lattice an O-point which is also an atomic site, resides within the center of the lattice $\vec{u_{O,1}} + \vec{u_{O,2}} = \left(\begin{smallmatrix} -1 \\ 2 \end{smallmatrix}\right)$. In order to find the correct coincidence site lattice from the O-lattice, the combination of O-lattice vectors have to chosen such that the coincidence site lattice has the smallest possible unit cell. This is done to ensure that the coincidence site lattice found from the O-lattice contains every coinciding lattice site. The corresponding coincidence site lattice can be found by:

$$\vec{u_{O,1}} + \vec{u_{O,2}} = \begin{pmatrix} -1 \\ 2 \end{pmatrix}, \vec{u_{O,1}} - \vec{u_{O,2}} = \begin{pmatrix} 2 \\ 1 \end{pmatrix} \tag{26}$$

Which will yield $\Sigma = \frac{\sqrt{(-1)^2+2^2}\cdot\sqrt{2^2+1^2}}{1} = \frac{1^2+2^2}{1} = 5$
The coincidence site lattice was found by using the subset of O-points that was also atomic sites, and while not every O-point is coincidence site point, every coincidence site point is an O-point. Unlike the coincidence site lattice, it is always possible to find an O-lattice provided one has the correct transformation operator which relates the two crystals lattices. If a configuration then has a coincidence site lattice, it may be found from the O-lattice as the coincidence site points are a subset of the coinciding equivalence points which are also lattice points.

4.2.2 General O-lattice theory

In the short example above, both lattices was square lattices. The rotation matrix which related the two lattices was defined for a rotation of the Cartesian coordinate system, which worked well in the example as the basis of both crystal lattices was an orthogonal basis. The situation would be more complicated if the basis of lattice A and B was in different basis than that of the square lattice. In addition the basis of lattice A need not to be same as for lattice B.

In order apply O-lattice theory to more general cases, one have to find the correct trans-

formation matrix M which properly relates lattice A with lattice B. In the short example we worked through above we had that the lattices we wished to relate both where square lattices, as such the coordinates of the vectors $\vec{r_A}$ and $\vec{r_B}$ are described in the Cartesian coordinate system, the only difference was that lattice B had was rotated by some angle with regards to lattice A.

In the case where the structure of the lattices A and B are different from that of a square lattice, a general rotation in the Cartesian coordinate system will not be able to describe the transformation relation between the two lattices. For example if the two base translation vectors of lattice A was given as $\vec{t_{A,1}}^{(Cartesian)} = \binom{1}{0}$, and $\vec{t_{A,2}}^{(Cartesian)} = \binom{cos(60)}{sin(60)}$, which in the coordinate system of the lattice will be $\vec{t_{A,1}}^{(A)} = \binom{1}{0}$, and $\vec{t_{A,1}}^{(A)} = \binom{0}{1}$, and lets say that lattice B is related to lattice A by a 60° rotation is the Cartesian coordinate system.
In the Cartesian coordinate system, the translation lattice vectors of lattice B would be $\vec{t_{B,1}}^{(Cartesian)} = \binom{cos(60)}{sin(60)}$, and $\vec{t_{B,2}}^{(Cartesian)} = \binom{cos(120)}{sin(120)}$, while in the coordinate system of lattice A they would be $\vec{t_{B,1}}^{(A)} = \binom{0}{1}$, $\vec{t_{B,2}}^{(A)} = \binom{-1}{1}$.
Therefore when expressing the equations and all the base translation vectors in the Cartesian coordinate system, the transformation between the two lattices only required a simple rotation matrix. Yet, when expressed the equations and base translation vectors in the basis of the coordinate system of lattice A, a simple rotation is no longer sufficient as the length of $\vec{t_{A,1}}^{(A)}$ is smaller than the vector $\vec{t_{B,2}}^{(A)}$ which we should obtain after operating with the transformation M.
The situation only becomes worse when the structure of lattice A and B also differs, as there are three different coordinate systems in which the equations may expressed in.
For reasons that will become clear later, it is a favourable to express the equations in terms of crystal coordinates. We will show how we can obtain a general formulation of M that takes into account the structure of the lattices.

$$x^{(A)} = S^{(A)} x^{(orth)} \tag{27}$$

Where the structure matrix $S^{(A)}$ is matrix that transforms an vector in an orthogonal coordinate system,$x^{(orth)}$, into a lattice vector of lattice A, $x^{(A)}$ expressed in an Cartesian coordinate system.
Such that $S^{(A)}\binom{1}{0} = x_1^{(A)}$, and $S^{(A)}\binom{0}{1} = x_2^{(A)}$, where $x_i^{(A)}$ is one of the basic lattice vectors of lattice A in Cartesian coordinates. Similarly we could do the same for lattice B.

$$x^{(B)} = RS^{(B)} x^{(orth)} \tag{28}$$

Here we have included a rotation matrix R in Cartesian coordinates, such that we are free to chose the orientation of lattice B.
By using that $x^{(orth)} = (S^{(A)})^{-1}x^{(A)}$ we may rewrite the equation as the following.

$$x^{(B)} = RS^{(B)}(S^{(A)})^{-1}x^{(A)} = Mx^{(A)} \tag{29}$$

This equation should be understood as for a lattice vector of lattice A, $x^{(A)}$ we may decompose it into a vector $(S^{(A)})^{-1}x^{(A)}$ whose entries corresponds to the number of lattice vectors of lattice A need to attain $x^{(A)}$.
Such that if $(S^{(A)})^{-1}x^{(A)} = \binom{\alpha}{\beta}$, the vector $x^{(A)}$, can be described by $\alpha \cdot x_1^{(A)} + \beta \cdot x_2^{(A)}$.
We then find the vector of lattice B, $x^{(B)}$ composed by the same combination lattice vectors but for lattice B by operating with $RS^{(B)}$.
Again it is worth mentioning that here the coordinates are expressed in the Cartesian coordinate system.
We mentioned earlier that it will become more useful to express the equation in terms of coordinates of the crystal lattices. Here we introduce the notation $x^{(0,A)} = x^{(A)}$, where the superscript $(0, A)$ refers to a vector of lattice A, expressed in Cartesian coordinates, and $x^{(C_A,A)}$ where the superscript (C_A, A) refers to the vector$x^{(A)}$ expressed the crystal coordinate system of lattice A.

We may rewrite any vector $\vec{x}^{(0,0)}$,Where the second entry in the superscript 0, refers to a general vector not necessarily associated with either crystal lattice, by

$$x^{(C_A,0)} = (S^{(A)})^{-1}x^{(0,0)} \tag{30}$$

Here we are to understand $x^{(0,0)}$ as a general vector in Cartesian coordinates, and $x^{(C_A,0)}$ as the same vector expressed in the coordinate system of lattice A. It is worth mentioning that earlier when we did this in equationwe used the same equation to perform a vector transformation, but here we are instead performing a coordinate transformation. In the same vein if we write:

$$x^{(0,0)} = S^{(A)}x^{(C_A,0)} \tag{31}$$

What is meant here is now that a vector in crystal coordinates of lattice A, is expressed in the Cartesian coordinate system by operating with $S^{(A)}$. We may express the equation 28 in the coordinate system of lattice A using these transformations as:

$$x^{(C_A,B)} = (S^{(A)})^{-1}x^{(0,B)} = (S^{(A)})^{-1}RS^{(B)}(S^{(A)})^{-1}x^{(0,A)} \tag{32}$$

which we again can rewrite as using equation 30:

$$x^{(C_A,B)} = (S^{(A)})^{-1} R S^{(B)} x^{(C_A,A)} = M^{(C_A)} x^{(C_A,A)} \tag{33}$$

Where $M^{(C_A)}$ is our new transformation matrix expressed in the coordinate system of lattice A. Which can be understood as we take a vector of lattice A expressed in the crystal coordinate of lattice A, and by operating with $RS^{(B)}$ we do vector transformation to get the corresponding lattice vectors of the B lattice in Cartesian coordinates, and finally we do a coordinate transformation to get the same vector expressed in the crystal coordinate system of lattice A. As we did earlier we find that if $x^{(C_A,B)} = x^{(C_A,A)} + t^{(C_A,A)}$ where $t^{(C_A,A)}$ is a translation vector belonging to lattice A in the coordinate system of lattice A, then $x^{(C_A,B)}$ is a equivalence point with $x^{(C_A,A)}$. We may then write:

$$x^{(C_A,B)} = M^{(C_A)} x^{(C_A,A)} = x^{(C_A,A)} + t^{(C_A,A)} = (M^{(C_A)})^{-1} x^{(C_A,A)} + t^{(C_A,A)} \tag{34}$$

$$(\mathbb{I} - (M^{(C_A)})^{-1}) x^{(C_A,A)} = t^{(C_A,A)} \tag{35}$$

Where we have introduced (C_A, O) as superscript referring to the fact these vectors describe equivalence points belonging to both lattices.

$$x^{(C_A,O)} = (\mathbb{I} - (M^{(C_A)})^{-1})^{-1} t^{(C_A,A)} \tag{36}$$

The solution to this equation will yield the O-lattice vectors expressed in the coordinate system of lattice A. Now we are seemingly almost done with the formulation of the transformation matrix, yet we have still will run into problems if we try to use this equation for any rotation. As an example, suppose both lattice A and B have a 60° rotational symmetry, and the structure matrix that produces the lattice A and B are given by:

$$S^{(A)} = S^{(B)} = \begin{bmatrix} 1 & cos(60°) \\ 0 & sin(60°) \end{bmatrix} \tag{37}$$

In this case the lattice produced by rotating lattice B by 60° yields the exact same lattice structure as if there was no rotation. Since every lattice site of A aligns perfectly with the lattices sites of B for $\theta = 0°$, and due to the six fold symmetry of lattice B this is also the case for a 60° rotation of lattice B. Therefore the O-lattice found by either $\theta = 0$ or 60°

should yield the same result. For a rotation by θ we find that

$$(M^{(C_A)})^{-1}) = (S^{(B)})^{-1}R^{-1}S^{(A)} = \begin{bmatrix} 1 & tan(60°)^{-1} \\ 0 & sin(60°)^{-1} \end{bmatrix} R(-\theta) \begin{bmatrix} 1 & cos(60°) \\ 0 & sin(60°) \end{bmatrix} \tag{38}$$

for $\theta = 0°$ we get that $(M^{(C_A)})^{-1}) = \mathbb{I}$, which makes sense as the structure matrices are the same and there is no misorientation between the two lattices. If we just insert into the equation it would tell us that there is no vectors of the O-lattice that connects the O-points, since every point in lattice A already physically coincides with its equivalence points in lattice B. In the case where $\theta = 60°$ we get instead:

$$M^{(C_A)^{-1}} = \begin{bmatrix} 1 & 1 \\ -1 & 0 \end{bmatrix}, and\, M^{(C_A)} = \begin{bmatrix} 0 & -1 \\ 1 & 1 \end{bmatrix} \tag{39}$$

When we insert this into our equation we find that the O-lattice vectors becomes ${x^{(C_A,O)}}_1 = \left(\begin{smallmatrix} 1 \\ -1 \end{smallmatrix}\right)$, and ${x^{(C_A,O)}}_2 = \left(\begin{smallmatrix} 1 \\ 0 \end{smallmatrix}\right)$. From ${x^{(C_A,O)}}_2 - {x^{(C_A,O)}}_1 = \left(\begin{smallmatrix} 0 \\ 1 \end{smallmatrix}\right)$, we can see that the O-lattice points are any points with integer value when expressed in the coordinate system of lattice A.

This means that the O-lattice we find produces the exact same structure as lattice A, and every lattice point of lattice A is therefore also an O-lattice point which must by the definition of the O-lattice also coincide with a lattice point from lattice B. But for the case of 60° misorientation should yield the same result as for the case with no misoritation, at least for this choice of structure matrices. We could have chosen to describe lattice B by $S^{(B)} = \begin{bmatrix} cos(60°) & cos(120°) \\ sin(60°) & sin(120°) \end{bmatrix}$, which would produce the exact same lattice as we used in our example, the only difference is in the choice of the base unit cell vectors.

Since the structure matrix we used in our example has a sixfold symmetry the we could have chosen any combination of $\left(\begin{smallmatrix} cos(60°\cdot n) \\ sin(60°\cdot n) \end{smallmatrix}\right)$ as the base vectors of the structure matrices, provided of course we do not chose a set of base vectors that run parallel to each other, and these would still produce the same lattice we considered in the example.

If we do the calculations the O-lattices in these cases, we find two categories of O-lattice, the first are of the type we calculated first for no misorientation, where there is no O-lattice vectors, the second are of the type we calculated for 60° misorientation, where the O-lattice contains every integer valued lattice point of lattice A. The reason we get a different results the case of 0° misorientation and for 60°, is that the transformation matrix that produces lattice B is formulated as an arbitrary point to point relation, which above a certain angle no longer accurately reflects the transformation relation between the structure of lattice A

and lattice B.
The same is also true for the different results we obtain for different choices of base lattice vectors, our choice of base lattice vectors does not change the structure of lattice B, but it does change the point to point relation between lattice A and B.
In addition there is no reason why we should limit ourselves to only performing rotations in order to produce an arbitrary oriented lattice B, we could just as well produce lattice B by operating with a pure shear matrix instead.

This leaves us with some ambiguity regards the formulation of the transformation matrix, as we must decide which choice of base lattice vectors, and what rotation or shear matrix will yield the correct O-lattice.
In regards to the two calculated examples in the case where $\theta = 60°$, we were able to find a O-lattice which connected every lattice point of A with a lattice point of B, while for $\theta = 0$ we found that there was no O-lattice.

We may be compelled to consider that the O-lattice found for $\theta = 60°$ was somehow more correct than the in nonexistent O-lattice found at $\theta = 0$, since we have found a lattice which tells us that every lattice point of A is coinciding with a lattice point of B.
Yet if we consider that from the lattice vectors of the O-lattice we should be able to reach every coinciding equivalence point of A and B, and since the structure of the lattice A is the exact same as that of lattice B every equivalence point should be an coinciding equivalence point. This we found not to be the case, as the only coinciding equivalence points was the lattice points of A and B.

Clearly for the case where lattices A and B have the exact same structure and the symmetrically same orientation, any result that would imply that the coinciding equivalence points are limited to only a finite set of points must be wrong as the there should be an infinite amount of sets of coinciding equivalence points.

The correct choice of transformation should always be the one that preserves the nearest neighbour relations, which mathematically corresponds to the transformation that produces lattice B given lattice A should minimize the numerical value of $|T| = |\mathbb{I} - (M^{(C_A)})^{-1}|$. While this is gives us a way to evaluate which of the possible transformations that produces lattice B should be the correct one, it requires that we already know every possible transformation matrix that could produce lattice B from lattice A.

We will present a method for obtaining a transformation matrix which should let us be able to calculate the correct O-lattice in most cases, though due to this ambiguity we can never be fully certain whenever the calculated O-lattice is the correct O-lattice. The procedure is as follows:

Given an arbitrary point to point relation ${M_{PtP}}^{(C_A)}$ between lattice A and B, where we have that:

$$x^{(C_A,B)} = {M_{PtP}}^{(C_A)} \vec{u_i}^{(C_A,A)} \tag{40}$$

Where we use the transformation ${M_{PtP}}^{(C_A)}$ to transform a unit vector from lattice A,$\vec{u_i}^{(C_A,A)}$, into a lattice vector from lattice B, $x^{(C_A,B)}$. Then from another transformation U we find the unit vector of lattice A which is closest to $x^{(C_A,B)}$.

$$\vec{t_i}^{(C_A,A)} = U\vec{u_i}^{(C_A,A)} \tag{41}$$

From the matrix U we attain our new unit cell for lattice A, which is closest to lattice vector $x^{(C_A,B)}$. Our intent is now to find the transformation which relates the lattice vector of B,$x^{(C_A,B)}$ to the closest unit vector from lattice A, $\vec{t_i}^{(C_A,A)}$. We may then write the following:

$$x^{(C_A,B)} = {M_{PtP}}^{(C_A)}(U^{-1})\vec{t_i}^{(C_A,A)} = {M_{NN}}^{(C_A)} x^{(C_A,A)} \tag{42}$$

Where we now have the transformation relating the nearest neighbours ${M_{NN}}^{(C_A)}$, now all we have to do is to find U.

We do have certain requirements for U, U must be unimodular as such $|U| = \pm 1$ such that it leaves the volume of the unit cell of lattice A unchanged while it may change the shape of the unit cell.
The procedure employed in this work, has been to find the distance between $x^{(C_A,B)}$, and the possible unit vectors of lattice A, expressed in the Cartesian coordinate system, in order to determine the which of the possible set of base unit cell vectors lies closest to the cell formed by the lattices vectors of B. In the case of there are multiple unit vectors that are closest to $x^{(C_A,B)}$, we make sure that the unit vectors chosen ensure that U is an unimodular matrix.

Now we have all what we need to calculate the O-lattice. For two arbitrary crystals A and B, we determine the structure matrices which produces these two lattices, and with the addition of a rotation we have a point to point relation between the two crystal lattices.
From this point to point transformation, and the possible base unit vectors of lattice A, we

can calculate U such that we may determine the transformation which accurately reflects the relation between structure of lattices A and B.

$$x^{(C_A,O)} = (\mathbb{I} - ({M_{PtP}}^{(C_A)}U^{-1})^{-1})^{-1}\vec{t}^{(C_A,A)} \tag{43}$$

With our previously somewhat arbitrary point to point transformation,
${M_{PtP}}^{(C_A)} = (S^{(A)})^{-1}R(\theta)S^{(B)}$.
Which we write for ease of reading as:

$$x^{(C_A,O)} = (\mathbb{T})^{-1}\vec{t}^{(C_A,A)} \tag{44}$$

Where $\mathbb{T} = (\mathbb{I} - ({M_{PtP}}^{(C_A)}U^{-1})^{-1})$. Since $\mathbb{T}^{-1}$ is a matrix whose columns are the O-lattice vectors, the determinant of $|\mathbb{T}^{-1}|$ will be the area or volume of the O-lattice in terms of the unit cell area of lattice A.
Meaning that the determinant $|\mathbb{T}|$ tells us how many O-points are contained within a single unit cell of lattice A, in other words it is the density of the O-points.

4.2.3 Solutions to the O-lattice

The solutions to this equation depends on the rank of $\mathbb{T} = (\mathbb{I} - (M_{PtP}{}^{(C_A)}U^{-1})^{-1})$. In the case of rank($\mathbb{T}$) = 3 we have that the solution yields a set of O-points that forms the 3 dimensional lattice, which we have dubbed the O-lattice.

Let us quickly refresh what is meant by an O-point.
For each point with an position in the lattice A there exists an point with an equivalent position in lattice B, these points are then equivalence points.
Furthermore each equivalence point is contained in a set of points reached by translations of the lattice vectors from the original equivalence point.
The O-points are the points for which the position of the equivalence point of lattice B is coinciding in real space, with a point from the corresponding set of equivalence points of lattice A.
An O-point is then a single point whose relative position within lattice A have the same relative position within lattice B. The solution for rank($\mathbb{T}$) = 3 tells us that the O-points we find forms a 3 dimensional lattice, i.e there exist only a discrete set of points within the 3dimensional lattices A and B for which the relative position in each lattice is identical.

Conversely for the case where rank($\mathbb{T}$) = 0, we have that lattice A and B perfectly coincides.
For this reason we can not find any discrete set of vectors that would yield all the possible O-points, as every point of lattice A and B, have the same relative position within each lattice and perfectly coincides and therefore every point in the space of lattice A and B is an O-point.
As such solution to the equation doesn't yield discrete O-points as the elements of our O-lattice but rather the elements of the O-lattice is an O-space.

In the case of rank($\mathbb{T}$) = 1 we have that there exists a single O-lattice vector for which every discrete O-point can be found.
This means that the relative position of points within lattice A and B only differs along continuous translations in the direction of the O-lattice vector. When the translation becomes an integer of the O-lattice vector, the relative position in A and B is the same.
Since for any translation normal to the O-lattice vector the relative position remains the same in both lattices, this means that at every discrete O-point, that we must have planes normal to the O-lattice vector for which every point in the plane is an O-point.
In other words, the solutions yields that the elements of the O-lattice are O-planes instead

of O-points.

At last for the case where rank($\mathbb{T}$) = 2 we have that there exists two O-lattice vectors from which we find a discrete set of O-points.
Just as before along the direction of either of the O-lattice vectors the relative position in A and B differs except at translations of integer combinations of the O-lattice vectors.
In this case we have that the discrete O-points are located within a 2 dimensional lattice spanned by the two O-lattice vectors.
For translations normal to both O-lattice vectors, the relative position in both A and B is the same. As such, for every O-point every point continuously along the direction normal to the two O-lattice vectors, is also an O-point.
Thus, rather than O-points the solution in this case would be that the elements of the O-lattice are O-lines.

In the examples presented so far we have exclusively worked with 2 dimensional lattices, yet we referred to the elements of our O-lattice as O-points instead of O-lines. Since a 2X2 matrix always will be of rank 2 or lower, the solution in our examples must have either yielded O-lattice with elements that are O-lines, O-planes or an O-space.

We will continue with the 2 dimensional description of the problem for now, and elaborate further on regarding the choice of dimension for the problem later on.

While we may solve the equation in the case where rank($\mathbb{T}$) = 2 with our 2 dimensional formulation of the problem, and find the O-lattice vectors there is still a little way to go before we are done.
First and foremost the O-lattice vectors we find do not necessarily correspond to a lattice site for either of the crystal lattices A, and B, this means that we have no guarantee that the O-lattice we find is periodic, or that there exits a coincidence site lattice but if it does exist it would have to be contained with the O-lattice.

4.2.4 Periodicity of the O-lattice

We may chose to split the coordinates of the O-points into its external coordinates and internal coordinates.

$$\vec{x}^{(C_A,O} = \vec{x}_{Ext}^{(C_A,O)} + \vec{x}_{int}^{(C_A,O)} \tag{45}$$

Where the external coordinate $\vec{x}_{Ext}^{(C_A,O)}$ refers to which cell of lattice A the O-point resides, and the internal coordinates $\vec{x}_{int}^{(C_A,O)}$ refers to the position within the cell the O-point resides. For obvious reasons the external coordinates can be written as an integer combination of lattice vectors of A, while the internal coordinates may assume any value in the range of $\{0 \leq \vec{x}_{Ext}^{(C_A,O)} \leq 1\}$.
When we gave our formulation of the O-lattice we aligned the origin of every coordinate system at a coinciding lattice point.
Since lattice points are located at integers of the lattice vectors, $\vec{0}$ therefore must always be coinciding lattice point regardless of the length and direction the lattice vectors of A and B. Since this choice of alignment always yields at the very least 1 coinciding lattice point we would like to keep this initial alignment, but we may change the origin of our coordinate system as we wish.
Furthermore if we had to change the initial alignment we would have to define entirely new transformation that takes into account the translation between the origin of lattice A and B, even if we find a coinciding site lattice for such, the same lattice structure would also be found in our initial choice of alignment.
Essentially the O-lattice we find would depend on the rotational alignment and the translational alignment of lattices A and B, while all the O-lattices which contains a coincidence site lattice only depends on the rotational alignment with no translational misalignment.

If we where to perform a translation of the origin of the coordinate system, the external coordinates would have to change, since they are defined with respect to the origin of the coordinate system, while internal coordinates would remain invariant as they are defined with respect to their relative position within a unit cell of lattice A.

For O-points which also belong to the coincidence site lattice, the internal coordinates must be $\vec{0}$.
If the lattice vectors of the O-lattice are the exact same as for a coincidence site lattice, i.e all O-points are also lattice points for both lattices A, and B, the O-lattice we find would have to be periodic.
Since we initially have a coinciding lattice site at our origin, we could move our origin of our coordinate system to an O-point of the coincidence site lattice, and the internal coordinates the origin would still have to be $\vec{0}$, as such the pattern remains the same.

On the Other hand if the solution yield that the O-points are not limited to lattice sites

of A and B, a translation of the origin by such an O-lattice vector would change the relative position of the origin within the unit cell of the crystal.
The internal coordinates of the origin has changed, and depending on the O-lattice, a new translation of the origin might result in another change in the pattern to either the original pattern, or a third entirely different pattern.

There is no reason for the O-lattice to be limited to 1,2 or 3 patterns, there may be an infinite amount of patterns within an O-lattice.

To determine the number of patterns contained within our O-lattice we introduce the reduced O-lattice.

This reduced O-lattice should be understood as a single unit cell of lattice A, for which the O-points of the regular O-lattice are located within the reduced O-lattice at their internal coordinates.
For O-points with the same internal coordinates the pattern remains the same, while for O-points with different internal coordinates the pattern would in turn differ as well.
Each individual pattern we call a pattern element, and there is as many pattern elements in an O-lattice as there is O-points in the reduced O-lattice.

If the O-lattice is periodic there must be a finite number of points in the reduced O-lattice, and the O-lattice for which all patterns are contained we denote as the full O-lattice.

If there where an infinite amount of points in the reduced O-lattice, it would mean that there must exist an infinite amount of patterns, meaning the full O-lattice would have to infinitely large in order to contain every pattern element, which means that there exits no periodic O-lattice.

We may calculate the number of pattern elements N, and while $N = \infty$ we can say that the O-lattice is not periodic, we cant say if an full O-lattice with $N = 2$ is more periodic than an full O-lattice with $N = 4$.

While N tells us how many pattern elements is contained within an full O-lattice it does not take into account the size of the O-lattice.

For example in the case where the structure matrices of A and B $S^{(A)} = S^{(B)} = \mathbb{I}$, with

$\theta = 36.87°$, we had that the O-lattice was

$$\mathbb{T}^{-1} = \begin{bmatrix} 0.5 & 1.5 \\ -1.5 & 0.5 \end{bmatrix} \tag{46}$$

In this case the O-points reached by either lattice vector of the O-lattice have the same internal coordinates $(0.5, 0.5)$, which means that a single translation of either lattice vector will reach the same O-point.
As such we only have 2 points in the reduced O-lattice $(0, 0)$ and $(0.5, 0.5)$, $N = 2$.

For the case where $S^{(A)} = S^{(B)} = \begin{bmatrix} 1 & cos(60°) \\ 0 & sin(60°) \end{bmatrix}$, we would find the following for $\theta = 21.88°$.

$$\mathbb{T}^{-1} = \begin{bmatrix} 1 & 3 \\ -3 & -1 \end{bmatrix} \tag{47}$$

Here the internal coordinates are $(0, 0)$ for the O-points reached by a single translation of either lattice vector.
As such there can only ever be 1 pattern element in this O-lattice. While equation 46 had two pattern elements, the corresponding coincidence site lattice area would be $\Sigma = 5$, while equation 47 only had one pattern element the corresponding coincidence site lattice area would yield $\Sigma = 7$.
We may define that area the full O-lattice N', which is the smallest lattice made of combinations of O-lattice vectors that contains all pattern elements, must have that the number of pattern elements can be found by

$$N = N' \cdot |\mathbb{T}| \tag{48}$$

Where $|\mathbb{T}|$ was the density of O-points per unit cell area of lattice A. In some cases it may be difficult to find which combinations of the O-lattice vectors will yield the full O-lattice, where as the produce we have to perform to find $|\mathbb{T}|$ and the number of pattern elements is very straightforward. If we assume that we can compute all pattern elements for a given O-lattice, we may rewrite this equation in order to find the area of the full O-lattice.

$$N' = \frac{N}{|\mathbb{T}|} \tag{49}$$

Here N' should give us a better measure of periodicity than N, since it tells how many unit cells of lattice A are needed in order to form a full O-lattice. This means that for low N' the full O-lattice repeats more often, and since that we have that for our choice of alignment

of the lattices A and B, where we remember that the origin of every coordinate system is a lattice point, the area of the periodic full O-lattice must always be an integer.
If this was not the case we would have the lattice vectors of the full O-lattice would have to not be integer vectors, since $N' = |\mathbb{T}^{-1}|$ but if that was the case a translation of from the origin to the O-point reached by an non integer vector would reach a different pattern element.

Since the full O-lattice is periodic every translation must reach the same pattern element, and since the origin is coinciding lattice site, every translation by vector from the full O-lattice must reach a coinciding lattice point.
As such we may note that the measure of coincidence for the coincidence site lattice, Σ would in most cases be equivalent to N'. This can be seen in the case where the rank of $\mathbb{T}$ was less than the dimensions of $\mathbb{T}$. In the case where $\text{rank}(\mathbb{T}) = 1$ we had that there was 1 O-lattice vector that reaches a set of discrete O-points, and a there was a plane where we had a continuous set of O-points. Since the set of continuous O-points can not be reached by any single discrete vector, the equation only yields the O-lattice vectors for the discrete O-points, yet within the continuous set of O-lattice points there may still exist a coinciding lattice site.

As such there may still be a coinciding site lattice with the dimensions of $\mathbb{T}$, despite that the equations would yield that $N' = \text{inf}$. The same is of course true for the case of $\text{rank}(\mathbb{T}) = 0$.

Since we would like to use O-theory to describe the interface-match between two arbitrary crystals, we are for now satisfied with the keep the problem entirely 2 dimensional.

5 Method and considerations

In this work we want to implement a model that uses O-lattice theory to calculate the interface match between 2 crystals. In 3 dimensions the O-lattice would give us a 3 dimensional lattice, while the interface boundary between the 2 crystals is a 2 dimensional plane. For the 3 dimensional O-lattice N' is not a measure of coincidence of a boundary but is instead a measure the coincidence between the 3 dimensional lattices that generate the O-lattice.
There may for example by a relatively low coincidence of the 3 dimensional crystal lattices, yet for the coincidence within an arbitrary boundary plane this might not be the case.
Furthermore the opposite may also be true, since the coincidence of the boundary depends on the coinciding lattice sites within the boundary, as such we need to define the relative orientation of interface plane we are interested in. We could choose a boundary plane with

a relative orientation fixed relative to the orientation of one of the crystals, and use the O-theory in 3 dimensions to calculate the interface match of the 2 dimensional boundary plane.

We would then have to determine which combinations of the O-lattices vectors belong to the interface boundary, which may not be entirely trivial. If we choose this approach we also have to determine which which plane of the other crystal, the interface boundary plane corresponds to.

If we on the other hand, choose to fix the interface boundary plane orientation relative to both crystals, such that we always have a clearly defined boundary plane, we may instead use O-lattice theory in 2 dimension. Since primarily interested with the interfacial match of two crystals at the contact interface, information regarding their match of the crystals 3 dimensional lattice is largely irrelevant. This simplifies the model as for the 2 dimensional approach, the O-lattice will always be contained within the interface boundary plane, unlike the 3 dimensional approach where we would have to determine which combinations of O-lattice vectors belonged to the interface boundary.

This approach requires us to then determine the structure matrices of each crystal, that produces the 2 dimensional lattices at the interface, where as for the 3 dimensional approach the structure matrices was invariant of choice of the boundary plane. In the 2 dimensional approach the plane of each crystal is fixed at the boundary, where we may use our 2 dimensional rotation matrix to change the relative in-plane orientation as we please.

For example lets say crystal A and B both are fcc crystals with the same lattice parameters, and crystal A has the (111) plane at the interface, and crystal B has the (110) plane at the interface.

In the 2 dimensional approach we may calculate the O-lattice for every choice of in-plane orientation of crystals A and B. If we wish to calculate the O-lattice for the case where A has the $(11\bar{2})$ plane at the interface, we would then need to determine the corresponding structure matrix before we may do so. In the 3 dimensional approach we only have to consider where we choose to orient our interface boundary plane with regards to lattice B, meaning that crystal B always have the same plane at the interface, while using 3 dimensional rotations we may orient crystal A such that we can find the O-lattice for the interface of a fixed plane of B with any plane of crystal A.

In essence the 3 dimensional approach would always to find interfaces matches between a specific plane of lattice B and any plane of lattice B, at the cost of introducing difficulties regarding determining the O-lattice of the two dimensional interface plane. The 2 dimensional approach is more convenient in regards to determining the O-lattice of the interface, while we are limited to specific interfaces where the planes of each crystal lattice are fixed at the boundary. In this work we have chosen to opt for the 2 dimensional approach due to it's convenience, while future work beyond the scope of this thesis should include a 3 dimensional treatment of the O-lattice.

Since we wish to numerically calculate the O-lattice finding every pattern element for a non periodic O-lattice would take an infinite amount of time since, there would be an infinite amount of pattern elements.
Furthermore if we perform a very small rotation while we are at a configuration with a highly coinciding O-lattice, the O-lattice of the new configuration would no longer be highly coinciding as we are not exactly at that orientation that gave us the "good" O-lattice.
As we may never reach exactly that orientation that results in configuration with a highly coinciding O-lattice we have much to gain if we introduce some fault tolerance in our implementation of the O-theory. The procedure for numerically calculating the pattern elements is done by subdividing the internal coordinates of the reduced O-lattice into a 100 cells. We initially calculate the two O-lattice vectors ${x_i}^{C_A,O} = \mathbb{T}^{-1}{t_i}^{C_A}$, from which we may find the O-points reached by combinations of these two O-lattice vectors.

$$\vec{x_{n,m}}^{(C_A,O)} = n\vec{x_1}^{(C_A,O)} + m\vec{x_2}^{(C_A,O)} \tag{50}$$

Where $(n, m = 0...10)$. We then find the internal coordinates of the O-point, such that if $\vec{x_{n,m}}^{(C_A,O)} = (5.21, -4.63)$ the internal coordinates are $(0.21, 0.37)$ as the positive remainders after subtracting interges. We then form an 10 by 10 matrix M, for which initially all entries are 0. The indices of M corresponds to the internal coordinates of the O-points, such that $M(1,1)$ would refer to the internal coordinates of $(0 \geq x < 1, 0 \geq y < 1)$, while the entries of M refers to whenever if we have an O-point present with these internal coordinates.

Here the O-point with internal coordinates $(0.21, 0.37)$ would result in that we set the entry $M(3,4) = 1$. If over the calculation we find that there exist another O-point with the internal coordinates corresponding to $M(3,4)$, the value of the entry remains as 1, since the value indicates if there is O-points occupying this set of internal coordinates, irregardless of

how many O-points occupies this entry.

When we have done this for each O-point, we may find the number of pattern elements by summing over the matrix elements of M.

$$N = \sum_{j=1}^{10} \sum_{i=1}^{10} M(j,i) \tag{51}$$

From which we may then find $N' = \frac{N}{|\mathbb{T}|}$.

In order to calculate the 2 dimensional O-lattice, we need the structure matrices that produces the lattices at the interfaces. Since we wish to use O-theory for any interface between 2 crystals, the lattice parameters need not be the same of each crystal.

For example let us say that we have that the structure matrix of crystal A and B at the interface plane is an square lattice, and have the same inplane orientation.

The only difference is lattice parameters, is $a_B = 1.01a_A$. In this case we would find that $a_B * 100 = 101a_A$, which means that the full O-lattice would be result in $N' = 101 * 101 = 10201$. Since there is only a 1% difference in the lattice parameters, we might instead say that $N' = 1$ with a strain of 1% along both its lattice vectors.
Since in general the lattice parameters of 2 crystals are not perfect fractions of small integers, we would want to set a threshold for which the lattice vectors of crystal A are allowed to strain in order find an O-lattice which is more periodic.

Suppose that we have two vectors $\vec{X_\alpha}^{(C_A,O)}$ formed by combinations of the base O-lattice vectors, which almost forms a full O-lattice, i.e a coincidence site lattice.

We may say that there exists a O-lattice wherein the vectors $\vec{X_\beta}^{(C_A,O)}$ which corresponds to those found for the unstrained O-lattice, forms a coincidence site lattice. We may write:

$$\mathbb{O}_{incomplete} = \mathbb{T}_{Init}^{-1} \cdot \begin{bmatrix} n_1 & n_2 \\ m_1 & m_2 \end{bmatrix} \tag{52}$$

Where $\mathbb{O}_{incomplete}$ is the matrix whose columns are the lattice vectors of the unstrained O-lattice that almost forms a full O-lattice. The full O-lattice can found by replacing $\mathbb{T}_{init}$ with $\mathbb{T}_{Strained}$ which includes the deformation of crystal B, or it could be obtained by rounding

the incomplete Lattice to the nearest integer since we are in the coordinate system of crystal A.

$$\mathbb{O}_{full} = \mathbb{T}^{-1}_{Strained} \cdot \begin{bmatrix} n_1 & n_2 \\ m_1 & m_2 \end{bmatrix} = \text{round}(\mathbb{O}_{incomplete}) \tag{53}$$

Where

$$\mathbb{T}_{Strained} = \mathbb{I} - (\mathrm{A}^{C_A}_{Strain})^{-1}, \text{Where } \mathrm{A}^{C_A}_{Strain} = {S^{(A)}}^{-1} \cdot R(\theta) \cdot S^{(B)} \underline{\sigma} U^{-1} \tag{54}$$

Where $\underline{\sigma}$ is a matrix that strains the lattice vectors of crystal B, such that we obtain a coincidence site lattice. This means that where $S^{(B)}$ expressed a lattice vector of crystal B in the Cartesian coordinates, the transformation $S^{(B)}\underline{\sigma}$ first deforms the lattice vector and then expresses that vector in Cartesian coordinates. We can then write:

$$\mathbb{I} - \mathbb{T}_{Strained} = (\mathrm{A}^{C_A}_{Strain})^{-1} \tag{55}$$

$${S^{(B)}}^{-1} R(\theta)^{-1} S^{(A)} (\mathbb{I} - \mathbb{T}_{Strained})^{-1} U = \mathbb{I} + \underline{\sigma} = \begin{bmatrix} 1+\epsilon_{xx} & \epsilon_{yx} \\ \epsilon_{xy} & 1+\epsilon_{yy} \end{bmatrix} \tag{56}$$

Using equation 53, we can obtain $\mathbb{T}_{Strained}$ by:

$$\mathbb{T}_{Strained} = (\mathbb{O}_{full} \cdot (\begin{bmatrix} n_1 & n_2 \\ m_1 & m_2 \end{bmatrix})^{-1})^{-1} \tag{57}$$

Now we have a method for calculating the deformation $\underline{\sigma}$ that we would have to include in order to for our O-lattice to form a smaller coincidence site lattice.

Firstly we have to determine whenever there exists O-points found by combinations of the O-lattice vectors, which are near a lattice site of crystal A. We have to ascertain whenever there could exist a full O-lattice before we can calculate how much the strain of the crystal lattice is needed to attain that O-lattice. If we find that there exists an O-point whose distance to the nearest lattice of A is within a set threshold, we save that O-point along with the values of (n, m) which produced that O-point. After doing this for every combination of $(n, m = -10...10)$, we may have a set of O-points which are within a threshold of a lattice site. We may find the closest lattice site of A by simply round Simply if:

$$threshold > |n\vec{x_1}^{(C_A,O)} + m\vec{x_2}^{(C_A,O)} - \text{round}(n\vec{x_1}^{(C_A,O)} + m\vec{x_2}^{(C_A,O)})| \tag{58}$$

Then we have that:

$$\vec{q_{n,m}}^{(C_A,O)} = \text{round}(n\vec{x_1}^{(C_A,O)} + m\vec{x_2}^{(C_A,O)}) \tag{59}$$

The vector $\vec{q_{n_1,m_2}}^{(C_A,O)}$ with the smallest deviation from lattice site, is the one we choose as one of the lattice vectors of the full O-lattice we would like to find. Now all we have to do is to find the second lattice vector. We first evaluate the determinant:

$$|\mathbb{T}_{[(n_1,m_1),(n,m)]}|^{-1} = det(\begin{bmatrix} \vec{x_{(n_1,m_1)}}_x^{(C_A,O)} & \vec{x_{(n,m)}}_x^{(C_A,O)} \\ \vec{x_{(n_1,m_1)}}_y^{(C_A,O)} & \vec{x_{(n,m)}}_y^{(C_A,O)} \end{bmatrix}) \tag{60}$$

If the determinant is zero it means that the lattice vectors run parallel or anti parallel to each other, as such we exclude these lattice vectors as possible solutions for the second lattice vector. We then find the vector $\vec{q_{n_2,m_2}}^{(C_A,O)}$ for which the determinant is non zero value, with the smallest deviation from a lattice site. There may be multiple lattice vectors that may have a larger deviation from a lattice of crystal A, for which $|\mathbb{T}_{[(n_1,m_1),(n_2,m_2)]}|^{-1} = |\mathbb{T}_{[(n_1,m_1),(n,m)]}|^{-1}$. Since these should all form the same coincidence site lattice structure, the $\underline{\sigma}$ needed to attain the necessary transformation should be the same. The same is of course also true for first choice of lattice vector as there should be many other choices of $\vec{q_{n_1,m_2}}^{(C_A,O)}$ for which we would obtain the same coincidence site lattice if we included the deformation.

As we may multiple possibilities regarding choice of lattice vectors, for sake of simplicity we choose that the lattice vectors should be those with the smallest length in the coordinate system of crystal B. In short we find two O-lattice vectors with the smallest deviation from a lattice site of crystal A, then find which other O-lattice vectors could produce the same coincidence site lattice, and choose the those with the smallest length in the coordinate system of crystal B.

We may be unable to find an O-lattice which is nearly a coincidence site lattice is this manner, and therefore we can not find a deformation matrix use to produce this coincidence site lattice as it does not exist.
While there it may not be possible to form a coincidence site lattice within the set threshold in this case, the computed value of N' might be a misleading low and close to an integer.
If this where to be the case as there is no deformation of crystal B, the code would output that N' corresponds to a reasonable periodic unstrained interface match. We have therefore implemented a similar procedure as the one above, to avoid this case. We calculate the

deviation from a integer of the base O-lattice vectors to a lattice site of crystal A.

$$\text{deviation} = |n_i \vec{x_i}^{(C_A,O)} - \text{round}(n_i \vec{x_i}^{(C_A,O)})| \tag{61}$$

We do this for $n_i = 1...10$ for both base O-lattice vectors. We then choose the values of n_i for which the deviations is assumes the lowest value, and use corresponding $\vec{q_{n_i}}^{C_A}$ as our lattice vectors of $\mathbb{O}_{full}$. This lets us calculate the deformation need to produce a coincidence site lattice, even if the deformation is considerably large and would lead to unfeasible interface matches.

The code [8] is done using MATLAB and to briefly summarize the model:

Using the relevant structure matrices of lattices A, and B as an input parameters, the model then computes the nearest neighbor transformation matrix for different rotations set within a range given as input parameter. From the nearest neighbor transformation matrix, the O-lattices is computed along with the deformation required to attain a full O-lattice according to the procedure set above. The deformation matrix is then converted into three parameters, ϵ_x, ϵ_y and $|\epsilon|$ where ϵ_i is the norm of the i'th column vector in $\underline{\sigma}$. As such the model doesn't differentiate between the geometric strain parallel to lattice vectors of B and the transverse strain. The sign of ϵ_i is determined by whenever the deformation would result in an increase or decrease in the length of the lattice vectors. The parameter $|\epsilon|$ is then the square root of square sum of ϵ_x and ϵ_y.

Finally the value of N' or Σ is computed, and the results are then sorted into tables, as to identify which rotations yields an full O-lattice where both the value of N' and $|\epsilon|$ is bellow a certain threshold set as an input parameter.

6 Results:Interface matching on a InAs Nanowire

In this section the model is utilized to find interfacial matches with Al and Pb on the side facets of hexagonal InAs nanowire. The nanowire considered in this sections are grown on an $(111)B$ InAs substrate, where the nanowires are grown along the $\langle 0001 \rangle$ direction. The resulting InAs nanowire then forms six $\{1\bar{1}00\}$ side facets, on which a film of either Al or Pb is grown.

We wish to use our model in order to provide qualitative answers on how the growth of Al (or Pb) film will depend on the structural properties of Al (or Pb) and the InAs. As a first step, we have consider which interfaces might have an impact on the growth kinetics.

Obviously the contact interface between Al(or Pb) with the $\{1\bar{1}00\}$ side facets are worth investigating. Furthermore for a low film thickness, the contribution to the excess chemical

potential from the top surface and substrate interface are the dominant factors in regards to grain growth along the surfaces of the nanowire.

As a starting point, the model calculates which orientations of a $\{h, k, l\}$ surface plane of Al or Pb would form interface matches on the $\{1\bar{1}00\}$ surface of the InAs, with a low value of N' corresponding to a coincidence site lattice, and with the least amount of geometric strain.

From the orientation of the grains provided by the interfacial match with the nanowire surface, the relative orientation between grains on the wires can be determined. The model is then applied in order to find which grain boundaries may occur based on the relative orientation between the grains.

For larger film thicknesses, the strain induced by the interface match, and grain boundaries are increasingly dominant in determining which preferred grain orientation would dominate the growth in the plane of the substrate surface.
Therefore ascertaining which grain orientation would minimize these factors allow us to superficially predict how the composition of thin film would evolve as the thickness of the film increases, and thereby which defects the model would expect to occur as a result.

With these results and from insight provided by the growth kinetics, we may provide qualitative answers to how the evolution of the film depends on the interfacial match.

6.1 Growth of Al film on InAs Nanowire

In the following subsections we consider the growth of film of Al on the hexagonal InAs nanowire. These have been experimentally made in work done by [9].

6.1.1 Al(h,k,l)/InAs $\{1\bar{1}00\}$ Interface match

To compute the interfacial match between the Al and InAs, we have to convert the (h, k, l) surface of Al, and the $\{1\bar{1}00\}$ surface of InAs into a 2 dimensional structure lattice that would produce the crystal structure of the boundary. The structure matrices can be found be choosing the 2 lattice vectors of crystal which belongs to the interface boundary, where we require that our choice of lattice vectors forms the smallest possible unit cell.

For the WZ phase of InAs, the two smallest lattice vectors in the $\{1\bar{1}00\}$ surface which produces the smallest unit cell are the lattice vectors along $[11\bar{2}0]$ and [0001]. The distance between In atoms along [0001] is 6.993Å, while the inter-atomic distance along $[11\bar{2}0]$ is

4.284Å. In this case the structural matrix for the $\{1\bar{2}00\}$ surface can then be written as

$$S_{InAs_{(1\bar{1}00)}} = \begin{bmatrix} 4.284\text{Å} & 0 \\ 0 & 6.993\text{Å} \end{bmatrix} = a_{InAs} \begin{bmatrix} 1 & 0 \\ 0 & c_{InAs} \end{bmatrix} \tag{62}$$

Where the lattice constant is $a_{InAs} = 4.284$Å, and $c_{InAs} = 1.633$ [10]. Here we have chosen to align the $[11\bar{2}0]$ direction along the Cartesian x-axis, and as a result the [0001] direction is align along the cartesian y-axis.

The structure matrix for the Al(h, k, l) surface will obviously depend on the out of plane orientation of the Al. We choose the (111) surface as our initial input, as the surface energy of the (111) facet is significantly lower than any other facet of Al. For the Al (111) plane we have chosen the lattice vectors along $[1\bar{1}0]$ and $[10\bar{1}]$ as the columns for the structure matrix. The inter-atomic distances in these directions are both $a_{Al} = 2.861$Å. The structure matrix is then given as:

$$S_{Al_{(111)}} = \begin{bmatrix} a_{Al} & cos(60°)a_{Al} \\ 0 & sin(60°)a_{Al} \end{bmatrix} \tag{63}$$

Where we have chosen to orient the $[1\bar{1}0]$ direction along the Cartesian x-axis, which as results in that the $[10\bar{1}]$ direction is oriented 60° from the x-axis. We may then write the arbitrary point to point transformation matrix $A(\theta)$ where we include a rotation of θ from the initial alignment, such that we are free to calculate the O-lattice for any choice of in plane alignment.

$$A(\theta) = (S_{Al_{(111)}})^{-1} R(\theta) S_{InAs_{(1\bar{1}00)}} \tag{64}$$

We insert these input parameters in our model and sweep over a range of $\theta = 0°$ to $\theta = 180°$ due to the two fold symmetry of the $\{1\bar{1}00\}$ plane, as to calculate the O-lattices at the interface between the Al $\{111\}$ surface with the $\{1\bar{1}00\}$ side facet of the InAs nanowire. The initial alignment of lattice planes are depicted in figure 4, along with the O-lattice found by that orientation. As we sweep over θ the lattice of the Al is rotated with respect to this initial alignment. Our finding are visualized in 5.

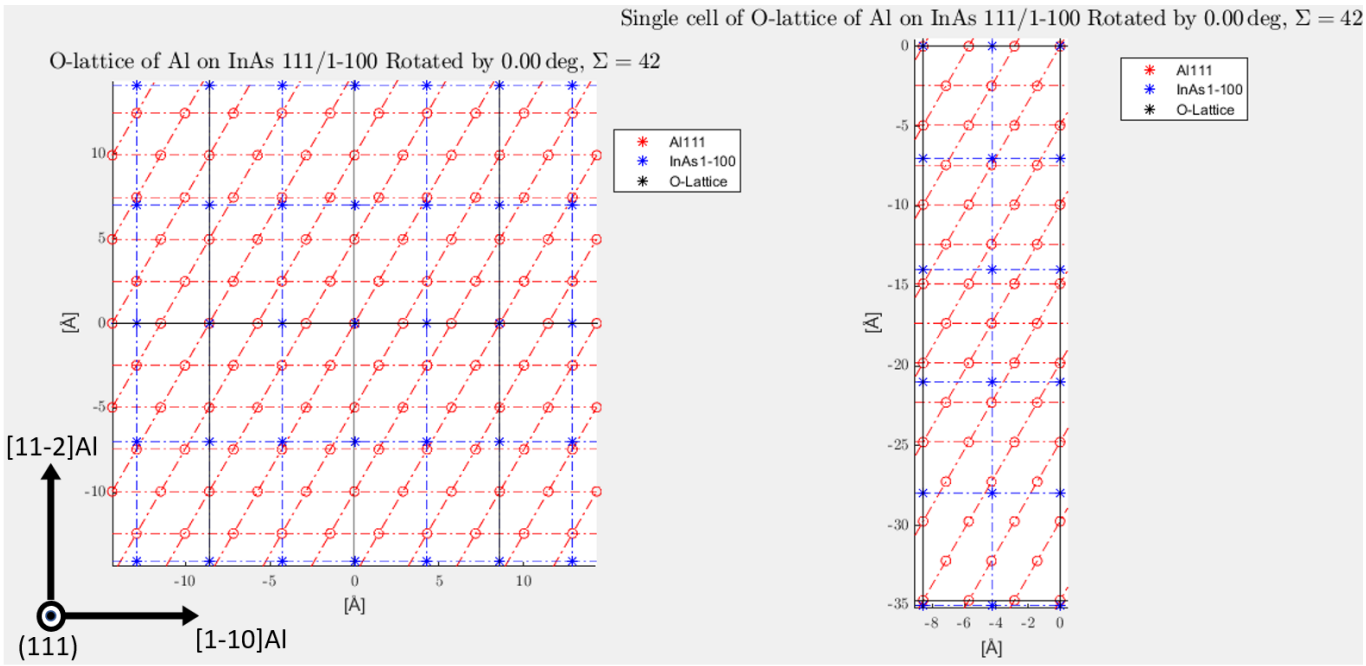

Figure 4: O-lattice found by the model for $\theta = 0°$ in black, in red $\{111\}$ surface plane of Al, in blue the $\{1\bar{1}00\}$ surface plane of the InAs nanowire.
The arrows in black indicate the orientation of the Al.
Left: broad view of the lattice planes of the Al and InAs
Right: View of a single cell of the O-lattice

Form figure 5 we may note that the 2 sets of columns which appears to form a full O-lattice without having excessively strain the crystal lattice. The first set of columns appears every $0 + n \cdot 60°$, and the other appears every $30° + n \cdot 60°$. These occur at $60°$ intervals due to the six fold symmetry of the $\{111\}$ plane. The values of the calculated Σ, and ϵ is shown in table 1

θ	Σ	ϵ	$\epsilon_{[11\bar{2}0]}$	$\epsilon_{[0001]}$
0°+60°n	42	0.85%	0.17%	-0.83%
30 °+60°n	60	2.8%	-1.33%	2.45%

Table 1: Calculated values of $\Sigma, |\epsilon|, \epsilon_{[11\bar{2}0]}, \epsilon_{[0001]}$ for θ

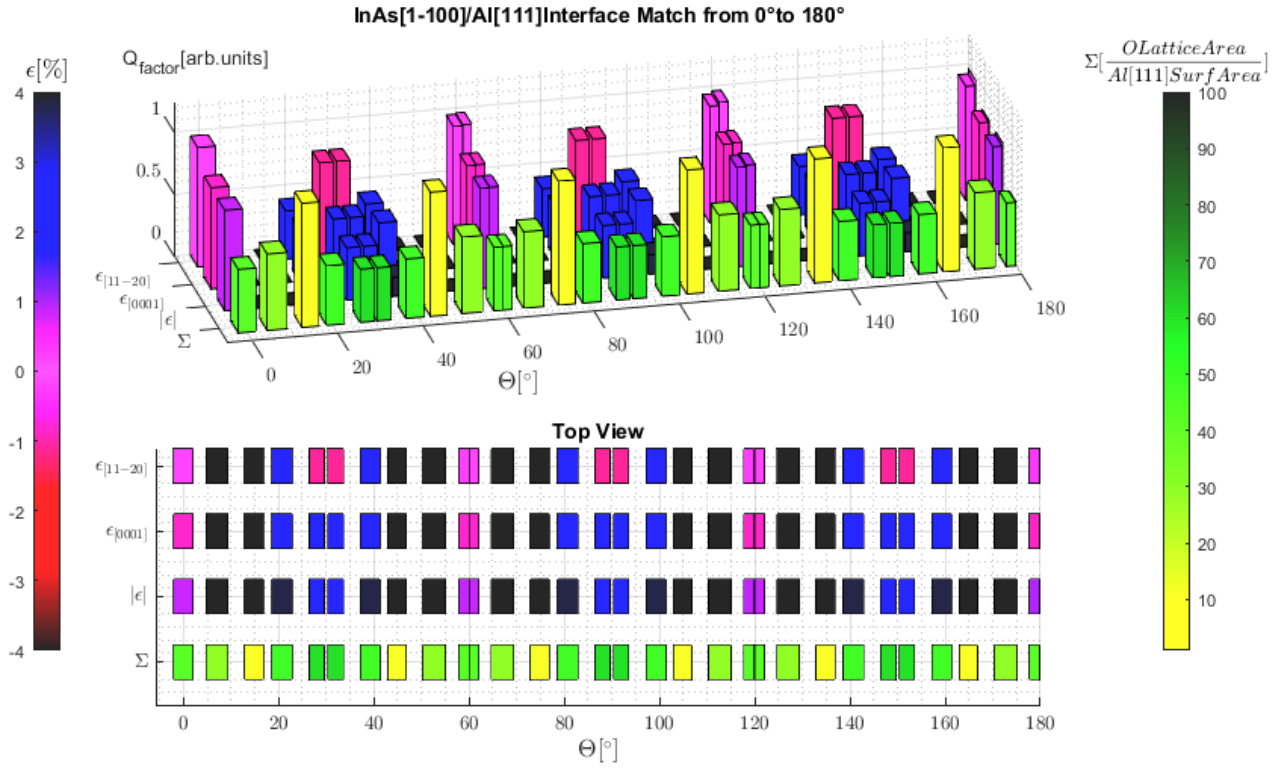

Figure 5: Various quantities calculated by the model represented as 4 columns
Top: Along the Y-axis in ascending order the type of quantity the columns represent, O-lattice area (Σ), Strain on InAs $[11\bar{2}0]$ ($\epsilon_{[11\bar{2}0]}$), and $[0001](\epsilon_{[0001]}$, and $|\epsilon|(\sqrt{\epsilon^2_{[0001]} + \epsilon^2_{[11\bar{2}0]}})$ The columns centered around certain values of θ along the x-axis in $^\circ$. The height of each column corresponds to a quality factor of quantity the column represents, with each quality factor defined differently, where a a quality factor of 0 is worst and 1 represents is best. The colorbar on the left side maps the value of strain to the columns that represents strain, while the colorbar on the right side maps the value of Σ to the column that represents Σ
Bottom: a top view of the column plot, for better view of values of each columns at the expense of losing the view of the quality factor.

The case for $\theta = 0° + 60°$ we find that the model tells that there is a $3[1\bar{1}0]Al$ to $2[11\bar{2}0]InAs$ with only 0.17% strain needed to achieve a coinciding lattice site. As such Al surface planes which contains the $\langle 1\bar{1}0\rangle$ lattice vectors may yield better interfacial matches. In the table 2 we have the calculated values for various choices of surface planes which all contains some of the $\langle 1\bar{1}0\rangle$ lattice vectors.

Table 2: Interfacial matches between a Al $\{h,k,l\}$ surface plane with the InAs$\{1\bar{1}00\}$, with the θ counting from the initial alignment of Al$\langle 1\bar{1}0\rangle$ along the InAs $\langle 11\bar{2}0\rangle$ direction

Surface plane of Al	θ	Σ	$\lvert\epsilon\rvert$	$\epsilon_{[11\bar{2}0]}$	$\epsilon_{[0001]}$
$\{001\}$	0°	15	2.24 %	0.17 %	2.23 %
$\{001\}$	15.99°	33	2.29 %	2.17 %	-0.76 %
$\{11\bar{2}\}$	0°	3	0.24 %	0.17 %	0.17 %
$\{11\bar{2}\}$	180°	3	0.24 %	0.17 %	0.17 %
$\{11\bar{2}\}$	44.41°	21	0.24 %	0.17 %	0.17 %
$\{11\bar{2}\}$	78.47°	15	0.25 %	0.17 %	0.17 %
$\{110\}$	0°	57	0.20 %	0.17 %	-0.10 %
$\{110\}$	70.53°	36	0.87 %	0.17 %	-0.85 %
$\{11\bar{3}\}$	0°	9	1.73 %	0.17 %	1.73 %
$\{11\bar{3}\}$	13.88°	51	0.30 %	0.21 %	0.22 %
$\{11\bar{3}\}$	33°	18	1.73 %	0.17 %	1.73 %

6.1.2 Al Grain boundary

For Al grains with a given out of plane orientation, the growth will initially favour the in plane orientation which minimizes the interface energy density from the interface between the grain and the underlying nanowire surface, i.e the in plane orientation which results in the best interfacial match. As the growth continues, the importance of the contributions of the interface between an Al grain grown on one of the six $\{1\bar{1}00\}$ facets, with the Al grain that resides on the neighbouring $\{1\bar{1}00\}$ facet, increases. In order to evaluate the interface match between and Al grain with a Al grain that resides on the neighbouring nanowire facet, we have to find two lattice vectors that connects coinciding atoms.

We limit ourselves to only look at matches between Al grains with the same orientation relative to the nanowire facet they reside on. As such the lattice vector along the length of the nanowire is the same, therefore we only need to find a lattice vector,$\vec{X}$ that connect coinciding atoms in the plane normal to the length of the nanowire.

To achieve this with our model we first find the structure matrix that produces the (h, k, l) plane that is aligned normal to the [0001] direction of the nanowire. In the case of the Al with the (111) out of plane surface, the plane normal to the [0001] direction would be the $(11\bar{2})$ plane. Similarly for the Al layer with the $(11\bar{2})$ out of plane surface, the plane normal to the [0001] direction would be the (111) plane.

We then use the structure matrix that produces the plane normal to the [0001] direction of the nanowire, and use that as our input in our model and set $\theta = 60^\circ$ to account from the difference in orientation since we are relating the Al layer with the Al layer on a neighbouring facet.

Below are a table of relevant values.

Interface plane	Surface normal to [0001]	$\vec{X}$ orientation [u,v,w]	Interatomic distance	ϵ_i	ϵ_j
(111) $\theta = 0$	$(11\bar{2})$	$[22\bar{4}9]$	97.62 **Å**	1.59%	-2.09%
(001) $\theta = 0$	$(1\bar{1}0)$	$[3\bar{5}0]$	11.79 **Å**	-3.36%	3.36%
$(11\bar{2})\theta = 0$	(111)	$[10\bar{1}]$	2.86**Å**	0%	0%
$(11\bar{2})\theta = 78.47°$	$(7\bar{5}1)$	[3 5 4]	28.6 **Å**	0%	0%
(110) $\theta = 0$	(001)	$[19 - 1\bar{1}0]$	44.4 **Å**	-0.24%	0.4%
$(110)\theta = 70.531°$	$(2\bar{2}1)$	[110]	28.6 **Å**	-2.86%	-1.65%
$(11\bar{3})\theta = 0$	(332)	$[11\bar{3}]$	26.8 **Å**	3.63%	-3.63%

Table 3: Table values; In column 1, Out of plane orientation of the Al grains, and in plane orientation. In column 2, corresponding the surface plane normal to the nanowire length In column 3, the orientation of the lattice $\vec{X}$ which connects coinciding lattice sites. In Column 4, the interatomic distance along the direction of $\vec{X}$ in order to achieve a coinciding lattice site. In Column 5, and 6, the strain required for to achieve this coinciding lattice site, with $\epsilon_{i(j)}$ defined as the strain along the first(second) lattice vectors of the structure matrices that produce the surface plane normal to the nanowire length.

We may note that for the case of an boundary between two adjacent Al grains with $(11\bar{2})$ orientation out of plane, the interface match was particularly good.

From our model we found that for a (111) plane related with a 60° rotated (111) plane the rank of $rank(\mathbb{T}(\theta = 60°)) = 0$ meaning that any lattice vector would reach a coinciding site.

In this case with the $(11\bar{2})\theta = 0$ orientation, the (111) plane is normal to the length of the nanowire, we found that a grain a could form a boundary with the grain b on the adjacent nanowire facet, with the following match $[111]_a/[111]_b$ and $[10\bar{1}]_a/[01\bar{1}]_b$.

Since our model is based on two dimensional inputs, we have neglected the exact structure of the crystal along the length of the nanowire. While we found that $rank(\mathbb{T}(\theta = 60°)) = 0$, this only tells us that we are free to choose any lattice vector along of the (111) plane as our boundary.
On figure 6 simulations made using VESTA[11], of the boundary is shown.

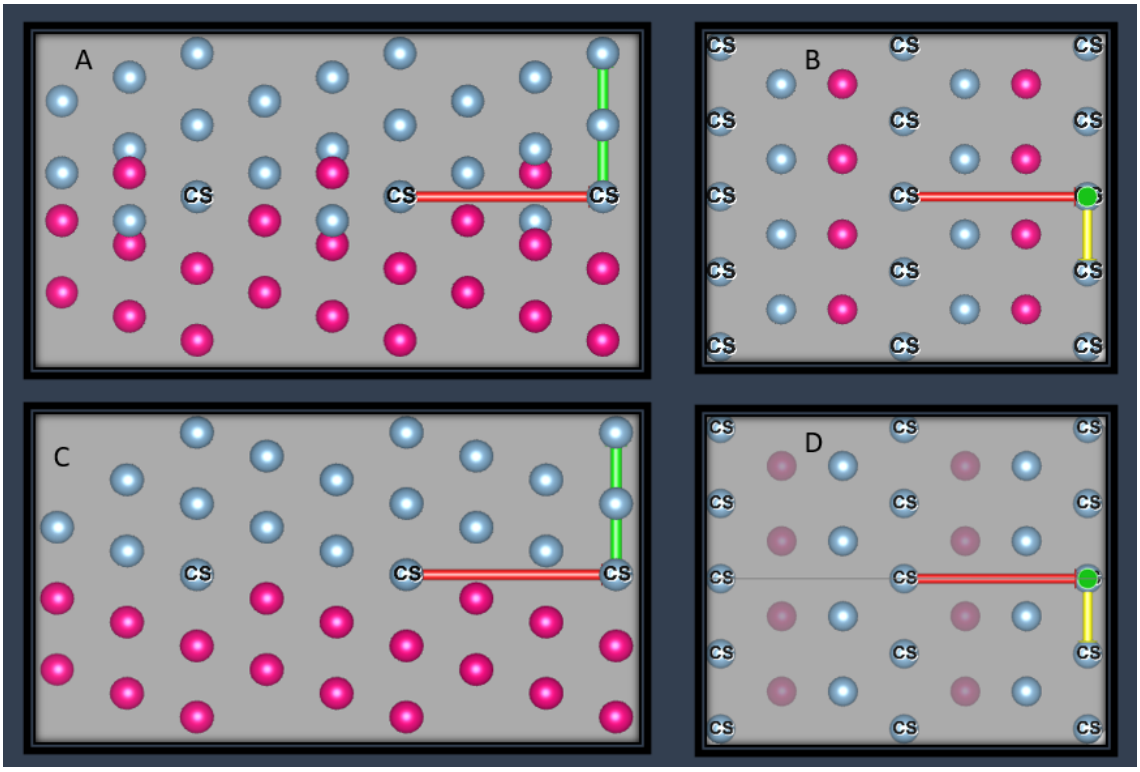

Figure 6: $[111]_a/[111]_b$ **and** $[10\bar{1}]_a/[01\bar{1}]_b$ **boundary between adjacent Al grains with** $(11\bar{2})$ **out of plane. Blue dots, corresponds to Al atoms of grain** a**, Red dots Al atoms of the adjacent grain** b**. The red line is the [111] direction relative to grain** a**, green line is the** $[1\bar{2}1]$ **direction relative to grain** a**, and the yellow line is the** $[10\bar{1}]$ **direction relative to grain** a**. The Atoms with the CS(coinciding site) label, are the atoms of the boundary witch are coinciding sites of both grains. On A, the boundary viewed from the** $[10\bar{1}]_a$ **direction, with a few atoms from each grain penetrating the boundary for visual effect. B, the boundary viewed from the** $[1\bar{2}1]$ **direction. C, and D, corresponds to the case where** $[\bar{1}\bar{1}\bar{1}]$ **direction of grain** b **is aligned in the same direction as the [111] direction of grain** a**.**

It should now be clear that the case of a boundary between two adjacent grain, both with $(11\bar{2})$ out of plane, and $\theta = 0$, the best boundary in terms of interface match was really a twin boundary.

Had we been doing the 3 dimensional O-theory approach on this configuration, we would have found that the solution to the fundamental O-lattice equation, would have yielded that the O-elements would have been O-planes. As such we have that every coordinate within (111) plane would be an O-point, with these planes spaced by the interatomic distance in the [111] direction.

Conversely, in the case of a boundary of two grains on adjacent nanowire facets, one with

the $(11\bar{2})$ out of plane surface, with $\theta = 0$, the other grain with $(11\bar{2})$ out of plane and $\theta = 180$, the boundary is particularly good. As shown in the C and D insets of figure 6, the structure of the grains on each side of the boundary are the exact same. if we had used the 3 dimensional O-theory approach our model would have yield that the O-elements in this case would have to be an O-space. This means that the structure of grain a simply continues into the structure of grain b, as such there can exist no grain boundary, and grain a and b instead just forms a single crystal.

In regards to grain boundaries between grains grown on the same nanowire facet, we have that for the $\{11\bar{2}\}$ out of plane orientation had as we mentioned in the previous subsection, two choices of in plane orientation which produced the same best interfacial match with the nanowire facet.

While the interface match had a two fold symmetry for a rotation around the $\langle 11\bar{2}\rangle$ orientation, the symmetry of the bulk structure is one fold for rotations around the $\langle 11\bar{2}\rangle$ orientation.
As such we have two variants of grains with the $\{11\bar{2}\}$ surface out of plane, which forms the same interface, with the same out of plane orientation. The first structural variant corresponded to the choice of aligning the [111] direction along the nanowire length with $\theta = 0$. The second structural variant corresponds to the case where $\theta = 180^\circ$ where the $[\bar{1}\bar{1}\bar{1}]$ direction was aligned along the nanowire length.

While the crystal structure of these variants differ along the nanowire length, both of these variants have the $\{111\}$ plane normal to the nanowire length. Therefore for a boundary between grains with the $\langle 11\bar{2}\rangle$ direction out of plane, if the structural variants differ they may form a twin boundary, if they do not differ they simply form a single crystal.

For grains with the $\langle 111\rangle$ out of plane orientations we had 6 choices of in plane orientations which also produced the same interfacial match with the nanowire facet.
While the interface match had a six fold symmetry for rotations around the $\langle 111\rangle$ direction, the bulk structure has a 3 fold symmetry for rotations around the $\langle 111\rangle$ directions. As such there can only exists two structural variants which produces the same interfacial match with the InAs facet, for $\{111\}$ surface out of plane. As before these may either form a twin boundary if the variants differ, or form a single crystal if the variants are the same.

6.1.3 Discussion:Al/InAs Nanowire

To interpret our findings in relation to how the interfacial match may affect the resulting composition of the growing Al film, and thereby which defects should arise, we consider two cases.

The first case is where the islands of Al merge and forms a thin film below a certain thickness. In this case the grains with an orientation that minimizes the contributions to the chemical potential from the out of plane surface and the Al/InAs interface, will grow at the expense of the grains with less favourable orientations. As such we would expect that the thin film would eventually be composed solely by grains for which the in plane growth conditions are most favourable.

Table 4: Surface energies of varous facets of Al [12]

Al facet	$\gamma_{(hkl)} eV/\text{Å}^2$
(111)	0.048
(322)	0.056
(100)	0.057
(332)	0.057
(221)	0.059
(311)	0.061
(110)	0.061
(211)	0.061
(210)	0.063

Since the (111) facet has the lowest surface energy of any facet of Al(see table 4, for the in plane growth to favour another out of plane orientation the interface match must at the very least be better than that for the (111) with the $\{1\bar{1}00\}$ surface of the InAs.

From our model we had that the best interfacial match of the (111) surface with a surface $\{1\bar{1}00\}$, was found by aligning the $[1\bar{1}0]$ direction along the $[11\bar{2}0]$ direction of the nanowire. This yield a value of $\Sigma = 42$, which required that we strained the lattice vector along $[11\bar{2}0]$ by 0.17%, and the lattice vector along [0001] by -0.83%.

The (110) surface of Al had a comparable interface match with $\Sigma = 36$, when we aligned the $[1\bar{1}0]$ $70.53°$ from the $[11\bar{2}0]$ direction, which required that we strained the lattice vector along $[11\bar{2}0]$ by 0.17%, and the lattice vector along [0001] by -0.85%. While in terms of

coincidence this interface is slightly better, it seems unlikely that the resulting decrease in interface energy would make up for the higher surface energy of the (110) facet when compared to the (111) facet.

On the other hand we found that the $(11\bar{2})$ surface of Al had the best interfacial match, $\Sigma = 3$, with the $\{1\bar{1}00\}$ surface of the InAs nanowire, with only a 0.17% strain on the lattice vector along the $[11\bar{2}0]$ direction, and 0.17% strain on the lattice vector along the [0001] direction. To decisively conclude whenever this interfacial match would mean that the $\{11\bar{2}\}$ out of plane direction would become the preferred orientation, we would have to calculate the resulting interfacial energy densities.

With the use of models such as density functional theory one may calculate the interface energy densities, but without such models it will be difficult to predict how the contributions from the Al/InAs interface compares to the contribution from the out of plane surface of the Al. The integration of such a model within our code is out of the scope of this thesis, as such our model can not ascertain whenever the interface match of $\Sigma = 3$ would have an interface energy which combined with the top surface contribution would be lower than the case for the (111) surface out of plane.

While we may can not with complete certainty determine which orientation would be preferred, we may consider two cases. For simplicity we assume that the area of the top surface of the Al grain increases at the same rate for the area of the contact interface with the InAs nanowire. If $\gamma_{(111)} + \gamma_{(111)/(1\bar{1}00)} < \gamma_{(11\bar{2})} + \gamma_{(11\bar{2})/(1\bar{1}00)}$ we would have that the $\{111\}$ surface out of plane would be the preferred orientation. The in plane orientation would then be the one which minimizes the interface energy, which we determined would have to be the one which aligned one of the $\langle 1\bar{1}0\rangle$ directions that belongs to the $\{111\}$ plane, along the $[11\bar{2}0]$ direction of the InAs.

As we mentioned earlier, there are two structural variants which forms the same interfacial match with the nanowire facet where the first structural variant was equivalent to aligning the $[11\bar{2}]$ direction along the [0001] direction of the InAs, the second structural variant was equivalent to rotating the first variant by 60° around the out of plane orientation. If two grains grown on the same facet have a different structural variant they may form a twin boundary, in this case the interface energy of this boundary will be $\gamma_{GB,(110)tilt} = 0.019eV/\text{Å}^2$ [13].Due to the degeneracy of the interface match, we should expect these two variants to form with the same probability. The energy density of this grain boundary may then con-

tribute to a driving force for the in plane growth as to eliminate these boundaries. Therefore along the length of the nanowire the {111} grains may form a strip of single crystals on the nanowire facet it resides.

Similarly if $\gamma_{(111)} + \gamma_{(111)/(1\bar{1}00)} > \gamma_{(11\bar{2})} + \gamma_{(11\bar{2})/(1\bar{1}00)}$, the grains with the $(11\bar{2})$ out of plane surface, would then grow at the expense of every other differently oriented grain. We determined that the in plane orientation which yields the best interfacial match would be the one which aligns the $\langle 1\bar{1}0\rangle$ of the $\{11\bar{2}\}$ surface along the $[11\bar{2}0]$ direction of the nanowire. As before we also have another structural variant which produces the same out of plane surface, and same interfacial match, which was equivalent to rotating the first variant by 180° around the $\langle 11\bar{2}\rangle$ out of plane orientation.

As before these two variants should form with the same probability, which again for adjacent grains of differing variants grown on the same nanowire facet, would form a twin boundary. In this case the interface energy of this grain boundary would be $\gamma_{GB,(111)twist} = 0.000eV/\text{Å}^2$ [13]. Due to this energy density we would not expect any driving force for the elimination of these boundaries. Therefore along the nanowire length the Al film on an $\{1\bar{1}00\}$ InAs facet, should be composed of many grains with the $\{11\bar{2}\}$ top surface.

As the thickness of the film increases, so too does the area of the boundary between the Al layer grown on one of the six $\{1\bar{1}00\}$ with the Al layer grown on the neighbouring facet. From our findings in table 3, we note that the best boundary plane between two Al layers with the (111) out of plane surface, was relatively bad.

The interatomic distance tells us that the height of the boundary need to be 97.6Å just to have one coinciding atomic site for both Al layers. In addition maintaining this boundary requires a significant amount of strain of the crystal lattice, $\epsilon_x = \epsilon_{[1\bar{1}0]} = 1.59\%$, and $\epsilon_y = \epsilon_{[11\bar{2}]} = 2.09\%$. As such we would expect that the boundary between Al layers (111), would be considerably unstable.

In all likelyhood the high interatomic distance, and large strain would probably mean that the calculated $(22\bar{4}9)$ boundary would never form. In addition the contribution to the chemical potential from grain boundaries between Al grains grown on the same facet, would likewise increase as the thickness of the Al layers increase.

On the other, for the Al grains $\langle 11\bar{2}\rangle$ out of plane orientation, the grain boundary between an Al grain with another Al grain grown on the neighbouring nanowire facet was particularly good.

In the case that the structural variants was the same, the boundary formed was a twin boundary with the interface energy $\gamma_{GB,(111)tilt} = 0.028eV/\text{Å}^2$ [13]. If the variants instead differed we found that there was no boundary so to speak, the structure of the Al grain could simply continue into the neighbouring grain. They therefore would then form a single crystal instead with no grain boundary and as such there would be no interface to contribute to the chemical potential.

Furthermore the interface energy of the grain boundary between different variants of Al grains on the same nanowire facet, was also incredible low $\gamma_{GB,(111)twist} =\approx 0eV/\text{Å}^2$. As such grain boundaries formed by variants of $\{11\bar{2}\}$ on the same nanowire facet, would not result in the $\{11\bar{2}\}$ grains becoming less favoured in regards to in plane growth as the thickness of Al layers increase.

We would therefore expect that as the growth continues the Al layers with $(11\bar{2})$ out of plane surface would be increasingly favoured by the in-plane growth.

If the case was that $\gamma_{(111)}+\gamma_{(111)/(1\bar{1}00)} > \gamma_{(11\bar{2})}+\gamma_{(11\bar{2})/(1\bar{1}00)}$, we would expect that growth in the initial stages favours the $\langle 11\bar{2}\rangle$ out of plane orientation, which as the thickness of the Al layers increases, becomes increasingly favoured.

As the thickness of the Al layers increase, the contribution from grain boundaries on the same nanowire facet have $\gamma_{GB,(111)twist} =\approx 0eV/\text{Å}^2$, as these boundaries wont result in the $\{11\bar{2}\}$ grains would be less favoured in regards to growth. As such we would expect that along the nanowire length, the structural variants will alternate and the boundary between them wont give rise to a driving force that may change this configuration.

The grain boundaries between Al grains of neighbouring nanowire facet, would if the structural variants change from facet to facet, form a single crystal. If the variants does not change from between facet to facet, a grain boundary forms with $\gamma_{GB,(111)tilt} = 0.028eV/\text{Å}^2$.

Therefore if the grain i is of the same variant as the grain j on the neighbouring facet,

and the grain k adjacent along the nanowire length is of a different variant, there will be a driving force for growth along the nanowire length, such that the grain k will grow at the expense of grain i in order to form a single crystal with grain j and thereby eliminating the $\gamma_{GB,(111)tilt}$ interface. As such we expect that a "ring" of six Al grains with alternating structural variants on the $\{1\bar{1}00\}$ facets, would grow along the nanowire length at the expense of neighbouring "rings" where structural variants does not alternate on between every facet. The driving force for this growth scales with the number of $\gamma_{GB,(111)tilt}$ interfaces, therefore we would expect that "rings" where every structural variant is the same, to be less common than "rings" with only a few $\gamma_{GB,(111)tilt}$ interfaces, which in term would be even less common than "rings" where the variants alternate between every nanowire facet.

In the opposite case, where $\gamma_{\{111\}} + \gamma_{\{111\}/\{1\bar{1}00\}} < \gamma_{\{11\bar{2}\}} + \gamma_{\{11\bar{2}\}/\{1\bar{1}00\}}$, we would expect that the growth initially favours the (111) out of plane orientation of the Al. As the thickness of the Al layers increase, the boundaries between Al grains on adjacent nanowire facets will result in that the $\langle 111 \rangle$ out of plane orientation becomes increasingly less favourable. Since this boundary was particularly bad as discussed earlier, there in all likelihood may never form a stable boundary.

There may be a possibility that the introduction of certain defects such as dislocations may allow the $\{111\}$ grains to form a less incoherent boundary, but the model in its current iteration does not include a method to determine whenever this might be the case.

From the results provided be our model we expect that it would be increasingly strenuous to maintain these boundaries as the thickness of the Al layer increases.
The instability of this boundary and maybe less importantly the strain induced by the interfacial match, may then provide the necessary conditions for the formations of Al grains with the $\langle 11\bar{2} \rangle$ out of plane orientation, and as for reasons we discussed above, would increasingly favored by the in plane growth.

As such we may expect that for some critical thickness, we would see a transition from $\langle 111 \rangle$ out of plane orientation, to the $\langle 11\bar{2} \rangle$ out of plane orientation.
As the $\{11\bar{2}\}$ top surface, lead to the formation of a single crystal between Al grains on adjacent nanowire facets, or twin boundaries, and had highly coincident interface with the nanowire facet, we would expect that this should translate in to a higher quality device performance. On the other hand the grains with the $\{111\}$ top surface, would result in unstable grain boundaries and a less coincident match with the InAs nanowire facets may lead to a reduction in device performance. As such it would be favourable to grow thicker films of

Al on the InAs nanowire in order to facilitate a transition such that the $\{11\bar{2}\}$ top surface would be the preferred grain orientation.

From experiments made by [9] we see that the initially the $\{111\}$ surfaces are dominating the in plane growth, which corresponds to the case where $\gamma_{\{111\}} + \gamma_{\{111\}/\{1\bar{1}00\}} < \gamma_{\{11\bar{2}\}} + \gamma_{\{11\bar{2}\}/\{1\bar{1}00\}}$. What we have neglected to mention is that the $\{11\bar{2}\}$ surface may form faceted surface which while increasing the surface area of the grain, leads to an decrease in total surface energy. In either case, despite the faceting of the $\{11\bar{2}\}$ surface, and the good interfacial match with the InAs $\{1\bar{1}00\}$ surface, the $\langle 111\rangle$ out of plane orientation is the most favoured by the in plane growth.

As the thickness of the Al layers increase, we see that there is transition from the planar $\{111\}$ surface to the faceted $\{11\bar{2}\}$ surface. This transition can be seen on figure 7, where the InAs nanowire is covered by planar $\{111\}$ Al shown a, which as the thickness increases transitions into the faceted $\{11\bar{2}\}$ Al shown in b, and c.

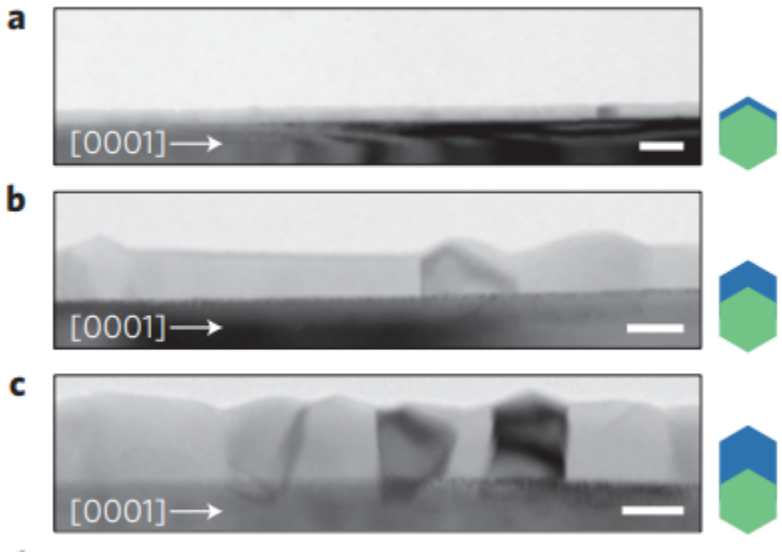

Figure 7: TEM image of Al grown on the side facets of an $[0001]_{WZ}$ InAs nanowire, at different stages of growth.

From figure 8 we see that there is two structural variantsα and β which are distinguishable by the TEM diffraction contrast. The formation of "rings" of single crystals is consistent with the results provided by our model.

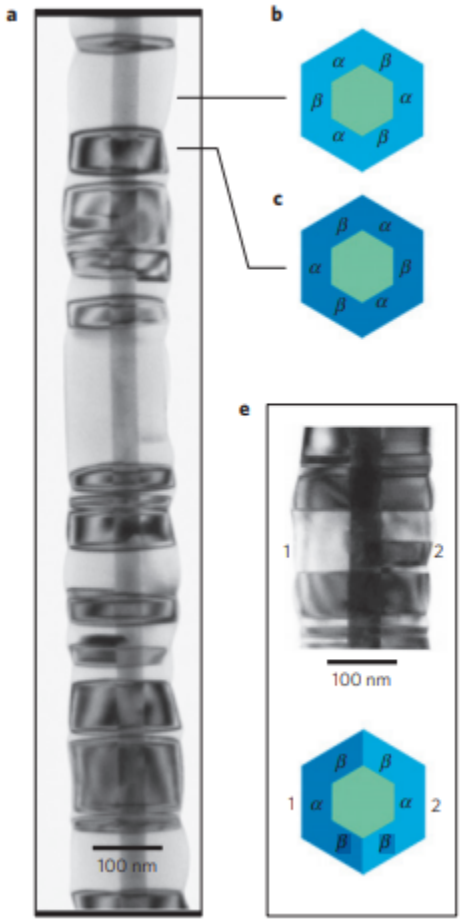

Figure 8: TEM image of an $[0001]_{WZ}$ InAs nanowire covered by Al taken from [9]

The dominant presence of "full-rings" indicates that may be a sufficient driving force for the elimination of the {111}tilt boundaries between grains on adjacent nanowire facets of the same structural variant. From insert e, however we can see that this driving force for may not be sufficient in the case of the "half-ring" in insert e. We may remember that contribution to chemical potential scales with the increase in change in shape parameter X with regards to a change in the number of atoms in the crystal n_p, $\delta\mu^X_{s-ERS} \propto \frac{\partial X}{\partial n_p}$.

In this case X would be the length of the Al grains along the nanowire [0001] direction $l_{[0001]}$, and $n_p = Area_{\{111\}} l_{[0001]}/\Omega_{Al}$, where $Area_{\{111\}}$ is the area of the $\{111\}$ plane normal to the nanowire length and Ω_{Al} is atomic volume of the Al.

This means that $\frac{\partial X}{\partial n_p} = \frac{\Omega_{Al}}{Area_{\{111\}}}$, as such the contribution to the chemical potential for growth along the nanowire length scales inversely with the area of the interface normal to the nanowire length. This means that the driving force for elimination of the boundaries

of adjacent grains of the same variant, is smaller if the grains forms a single crystal with the other adjacent grains. Since we may either have 0,2,4 or 6 of these {111} tilt boundaries depending on how the variants alternate on the nanowire facet, the driving force for eliminating those boundaries should be lowest if we have two boundaries which maximizes the area of the interface normal to the nanowire length, which is the case for the "half-ring" configuration.

From intuition we would then infer that nanowires with a larger width would increase the area of the interface normal to the nanowire length, which in turn would lead to lower driving force for the elimination of the {111} tilt boundaries, and vice versa.
Furthermore, the area of the {111} interface normal to the nanowire length may increase at a different rate than the area of the interface with the {111}tilt boundaries for increasing Al layer thickness, as such there may exist a regime for where the driving force for elimination of the {111}tilt boundaries is sufficient enough to disallow the "half-ring" configuration.

On the other hand there may also exist regimes wherein the driving force insufficient such that there may form other configurations than just the "half-ring".

Modelling the relevant growth kinetics may allow us insight in under which conditions these regimes may exist, such that by controlling the growth rate of the thickness of the Al layers, depending on the width of the nanowire, we may eliminate the formation of the {111}tilt boundaries in order to achieve higher quality devices.

6.2 Growth of lead film on InAs Nanowire

In this section the model is utilized in a similar case as the previous, where Pb is the material grown on the hexagonal InAs nanowire. While the crystal structure of lead is quite similar to Al, the difference in lattice parameter leads to wildly different results. This nanowire devices was experimentally made in work done by [14]. As before we initialize our findings by first calculating the interfacial match of lead with the side facets of the InAs nanowire.

6.2.1 Lead(h,k,l)/$\{1\bar{1}00\}$ Interface match

We consider the interface match between lead(Pb) as an fcc crystal. Here the structure matrices are almost the same as for Al the only difference is in the lattice constant.

Table 5: Calculated values for various out of plane orientation for the match between Pb and InAs$\{1\bar{1}00\}$, with Pb$[1\bar{1}0]$ direction oriented along the InAs $[11\bar{2}0]$ direction

Out of plane	θ	Σ	$\lvert\epsilon\rvert$	$\epsilon_{[11\bar{2}0]}$	$\epsilon_{[0001]}$
[111]	0°+n·60°	77	1.46 %	-0.13 %	1.45 %
[111]	0°+n·60°	35	2.64 %	2.15 %	1.45 %
[111]	30°+n·60°	48	0.12 %	-0.09 %	0.08 %
[111]	30°+n·60°	28	1.01 %	-0.97 %	0.31 %
[110]	20.47°+n·180°	78	0.17 %	0.16 %	0.08 %
[110]	90°+n·180°	12	0.93 %	-0.95 %	0.08 %
$[11\bar{2}]$	0°+n·180°	99	0.31 %	-0.12 %	0.08 %
$[11\bar{2}]$	11.25°+n·180°	10	0.12 %	0.09 %	0.09 %
$[11\bar{2}]$	45.58°+n·180°	14	0.11 %	0.08 %	0.08 %
[001]	0°+n·90°	22	0.17 %	-0.13 %	0.09 %
[001]	20.81°+n·90°	17	0.77 %	-0.53 %	0.37 %
$[11\bar{3}]$	90°+n·180°	28	0.17 %	-0.15 %	0.08 %

From table 5 the best interfacial match in terms of coincidence is found for grains with the $\{11\bar{2}\}$ top surface, with $\theta = 11.25°$.
In terms of geometric strain the interface of the InAs facet with a grain with the $\{11\bar{2}\}$ top surface where $\theta = 45.58°$, yielded the least geometric strain, though only by a very small margin.

For most out of plane orientations of a grain, an reasonable interface match could be found. with a low amount of geometric strain needed to achieve this interface match.

For grains with the $\{111\}$ top surface, the best interfacial match with the InAs was found by $\theta = 30°$. In this case two interfacial domains may be formed, one with a low amount of geometric strain but less coincident, and one with smaller interface domain and therefore more coincidence at the cost of a larger amount of geometric strain needed to achieve this match.

From these interfacial matches we find the in plane orientation for a fixed out of plane orientation that yields the best interfacial match.

For the two grains with same out of plane orientation and in plane orientation relative to to nanowire facet they reside on, the lattice vector along the [0001] direction of the InAs nanowire is of same length.
Therefore an possible grain boundary between grains of adjacent nanowire facets can be found by finding a single coincidence site lattice vector for the lattice plane of the grains normal to the nanowire length. In table 6 the results are shown, for certain choices of out of plane orientations and in plane orientations which yield the best interfacial match in table 5.

Interface plane	Surface normal to [0001]	$\vec{X}$ orientation [u,v,w]	Interatomic distance	ϵ_i	ϵ_j
(111) $\theta = 30°$	$\{1\bar{1}0\}$	$\langle 001 \rangle$	19.80 **Å**	1.75%	1.78%
(110) $\theta = 90°$	$\{1\bar{1}0\}$	$\langle 001 \rangle$	19.80 **Å**	1.75%	1.78%
$\{11\bar{2}\}$ $\theta = 11.25°$	$\{354\}$	$\langle 2\bar{3}, 25, \bar{1}4 \rangle$	123.80 **Å**	-4.33%	-2.54%
$\{11\bar{2}\}$ $\theta = 45.58°$	$\{1\bar{9}\bar{4}\}$	$\langle 120 \rangle$	28.30 **Å**	1.18%	5.92%
(001) $\theta = 0°$	$\{1\bar{1}0\}$	$\langle 001 \rangle$	19.80 **Å**	1.75%	1.78%
$\{11\bar{3}\}$ $\theta = 90°$	$\{1\bar{1}0\}$	$\langle 001 \rangle$	19.80 **Å**	1.75%	1.78%

Table 6: Table values; In column 1, Out of plane orientation of the Al grains, and in plane orientation. In column 2, coresponding the surface plane normal to the nanowire length In column 3, the orientation of the lattice $\vec{X}$ which connects coinciding lattice sites. In Column 4, the interatomic distance along the direction of $\vec{X}$ in order to achieve a coinciding lattice site. In Column 5, and 6, the strain required for to achieve this coinciding lattice site, with $\epsilon_{i(j)}$ defined as the strain along the first(second) lattice vectors of the structure matrices that produce the surface plane normal to the nanowire length.

What is note worthy is that aside from grains with the $\{11\bar{2}\}$ top surface, the best interfacial match was found by aligning the $\langle 1\bar{1}0 \rangle$ direction along the [0001] direction of the InAs nanowire.

Therefore grain boundaries between grains with the $\langle 1\bar{1}0\rangle$ along the nanowire length, belongs to the set of grain boundaries found by a rotation around a $\langle 1\bar{1}0\rangle$ axis. Unfortunately in this case there does not exist a coincidence site lattice configuration for a misorientation by 60° without introducing significant strain.

The best coincidence site lattice for a 60° misorientation, yielded $\Sigma = 20$ with $|\epsilon| = 2.50\%$, where the shortest vector of the coincidence site lattice, yielded an inter-atomic distance of 19.80Å. Like wise, the $\{11\bar{2}\}$ top surface has no good coincidence site lattice for the lattice planes normal to the nanowire length when there is a 60° misorientation. Despite ,in terms of coincidence the $\{11\bar{2}\}$ top surface had the best interfacial match for $\theta = 11.25°$, the possible grain boundaries between grains on adjacent nanowire facet was found to be the worst of those in table 6.

6.2.2 Discussion:Lead/InAs Nanowire

While the film thickness of the Pb film is small, the dominant contribution to the driving force for growth in the plane of the nanowire facet is those from the top surface of the grains and the substrate interface.

In table 7 a list of surfaces planes of Pb, and the associated surface free energy density for that surface plane.

As before, the $\{111\}$ surfaces planes have the lowest surface free energy density, meaning that grains with the $\{111\}$ top surface, without considering the interface match, should growth at the expense of other grains within the film. Like the case discussed in the earlier section,the $\{11\bar{2}\}$ top surface had the best interfacial match in terms of both geometric strain and coincidence, though in this case only marginally so.

Unlike the previous case, in order to achieve this match the in plane alignment that yielded this match was found by $\theta = 11.25°n \cdot 180°$.
The question is then whenever grains with the $\{11\bar{2}\}$ top surface and this interface match, or grains with the $\{111\}$ top surface and the interface match found at $\theta = 30°$, would minimize the overall contributions from the top surface and substrate interface.
The interface energy density from the substrate interface should in general be lower than the surface free energy of the corresponding lattice plane. Therefore it would be more likely that the grain orientation that minimizes the contribution from the top surface would dominate the growth over the plane of the nanowire facet.

As the thickness of the film increases the contribution from strain and the grain boundaries becomes increasingly important.
In regards to strain induced by the interface match, for both the $\{111\}$ top surface and $\{11\bar{2}\}$ top surface, the interface match yielded a nearly negligible amount of geometric strain in order to achieve the best interfacial match with the InAs nanowire facet.

In regards to grain boundaries, since as before the interface match of between the $\{11\bar{2}\}$ plane of Pb with the $\{1\bar{1}00\}$ facet of the InAs nanowire, had a two symmetry for rotations around the $\langle 11\bar{2}\rangle$ direction normal to interface plane, while the bulk crystal structure had a one fold symmetry. This corresponds to two distinct structural variants of grains with a $\{11\bar{2}\}$ top surface, the same is also true of grains with the $\{111\}$ top surface.
These structural variants should then be equally favoured by the growth along the plane of the nanowire facet, while the film thickness is small. Boundaries between different structural variants of grains on the same nanowire, may form twin boundaries, as the crystal structure in the plane of the nanowire facet, and the lattice vector directly normal to the substrate interface is the same.

For grains with the $\{111\}$ top surface, the boundary between different variants corresponds to a tilt boundary caused by a rotation around the [111] axis, with $\gamma_{[111]tilt,Pb} = 0.015eV/\text{Å}^2$ [13]. Like wise twin boundaries between grains with the $\{11\bar{2}\}$ top surface corresponds to the a twist boundary caused by a rotation around the [111] axis with $\gamma_{[111]twist,Pb} = 0.004eV/\text{Å}^2$ [13].

For grain boundaries between grains on different nanowire facets, we saw that in table 6 there wasn't any one good boundary with requiring an large amount of geometric strain.

Therefore it may be that the inclusion of another grain that occupies the small wedge at the corner of between the nanowire facets, could form two coherent grain boundary with the both grains on nanowire facets that surrounds the wedge.

This would increase the amount of grain boundaries between two grains on adjacent nanowire facets, from one to two, while it may result in an overall decrease in the contribution to the chemical potential from the grain boundaries.

Both grains on the adjacent nanowire facets have the same $\{h, k, l\}$ plane normal to the

length of the nanowire, with a difference 60° rotation around the axis normal to the $\{h, k, l\}$ plane.
The wedge grain also has the same $\{h, k, l\}$ plane normal to the length of the nanowire, with rotation around the axis normal to the $\{h, k, l\}$ plane by Θ_W.

As such for the wedge grain to form coherent grain boundaries, we must have that a rotation of the $\{h, k, l\}$ plane by θ_W and $60° + \theta_W$ both yields an coincidence site lattice.

For the grains on the nanowire facet with the $\{111\}$ top surface for the best interfacial match had the $\{1\bar{1}0\}$ plane normal to the nanowire length. For $\theta_W = 70.53°$ a coincidence site lattice with $\Sigma = 3$ is attained, while $\theta_W + 60° = 130.53°$ yields a strained coincidence site lattice with $\sigma = 42$.

Furthermore, a rotation by 129.53 degree would yield a coincidence site lattice with $\Sigma = 11$. Since this coincidence site lattice configuration is within 1° from what our model outputs, it may very well be that at the cost of some strain, it is possible for the wedge to form a twin boundary with one grain on a nanowire facet, and a strained $\Sigma = 11$ boundary with the grain on other nanowire facet.

For the grains on the nanowire facet with the $\{11\bar{2}\}$ top surface for the best interfacial match in terms of strain had the $\{1\bar{9}\bar{4}\}$ plane normal to the nanowire length, and best interfacial match in terms of coincidence had the $\{354\}$ plane normal to the nanowire length.

From the output of our model, we are unable to find any θ_W which could form an coincidence site lattice for both θ_W and $\theta_W + 60°$ even with some leeway in regards to geometric strain.

As such we would expect that grains with the $\{111\}$ top surface may form wedges that would lower the overall energy of the grain boundaries, while grains with the $\{11\bar{2}\}$ top surface would form incoherent grain boundaries.

Therefore we would expect that grains with the $\{111\}$ top surface would increasingly dominate the growth along the surface of the nanowire as the thickness of the film increases.
Furthermore, the grain boundary energy density from the boundaries between different variants of grains along the length of the nanowire, was quite large $\gamma_{\{111\}tilt} = 0.015eV/\text{Å}^2$.

Therefore the growth may strive to eliminate these boundaries and form a single crystal along the length of the nanowire.

We would therefore expect the film of Pb to form a single crystal along the length of the nanowire, with the {111} top surface, and the $\{1\bar{1}0\}$ plane normal to the [0001] direction of the InAs nanowire. Further more we would expect the formation of single crystal wedges along the length of the nanowire, between adjacent nanowire facets.
These wedges form twin boundaries with the strip of Pb from one facet of the nanowire, and a strained $\Sigma = 11$ boundary with the strip of Pb on the other nanowire facet.

Due to energy density of the {111} surface of Pb this should be the grain orientation at any point during growth, and due to the coherent grain boundaries formed by the introduction of the wedge grain this composition should also be the preferred orientation for larger thicknesses of the Pb film.

If the growth would result in single crystal strips on the $\{1\bar{1}00\}$ side facets along the length of the nanowire, which may be beneficial in terms of device quality. Therefore the only grain boundaries formed should be the coherent grain boundaries formed by the introduction of a wedge grain. While in comparison to single crystal with no grain boundaries, the grain boundaries of the wedge grain may serve as defects witch may reduce the overall device quality, but compared to the gain in device performance from not forming any axial grain boundaries, this may be negligible effect.

Table 7: Surface energies of various facets of Pb [12]

Pb facet	$\gamma_{(hkl)} eV/\text{Å}^2$
(111)	0.016
(322)	0.018
(100)	0.020
(332)	0.018
(221)	0.018
(311)	0.021
(110)	0.021
(211)	0.019
(210)	0.022

7 Future work

The model as implemented in its current iteration allows us to find interfacial matches between different crystals. The usefulness of the model is limited by its 2 dimensional formulation, as we have to choose which lattice plane of the crystal structure for which we hope to find an interface match. As such future work should include a model utilizing the 3 dimensional approach to O-theory. Aside from O-lattice theory there are methods for interface matching [15], which may be better suited to find orientations of two materials which would result in highly coincident and low strained interfaces. Furthermore, O-theory does also provide framework for calculating a lattice of dislocations which preserves the boundary. We did not discuss this feature of O-theory, as the implementation within the current model was out of the scope of this thesis. For the same reason, research of this feature of O-theory was rather limited, as such without the exact details whenever this application of O-theory will yield useful results remains to be determined. Even then, the usefulness of purely geometrical model would still be limited by its inability to provide more quantitative results. As we saw in the case of growth of an Al film on an hexagonal InAs nanowire, to model found an highly coincident interface of the $\{11\bar{2}\}$ surface of Al with the $\{1\bar{1}00\}$ surface of InAs. In addition the formation of grain boundary defects was limited to twin boundaries, and the formation of a single crystal between the grains on the side facet was possible. This should translate into a higher quality device performance, but since the composition of the film is determined by energetics and not geometry, for low thickness the $\{111\}$ top surface was the preferred orientation. In order to accurately determine which interfaces would lead to stable interfaces with few grain boundary defects, we also have to determine which orientations would be preferential in terms of growth kinetics.

The goal for futher work could thus entail: the creation of software, which can identify the material combinations and the relative orientations which may form stable interfaces based on a geometrical approach. This should include method for dynamically calculating which boundaries may arise as result of an interfacial match. When the model has found which grain orientations would lead to stable boundaries based purely on geometric considerations, another module should simulate the relevant growth kinetics such that we may determine whenever the energetics allow for this desired outcome to happen, and if which growth conditions/film thickness,temperature,vapour pressure etc.) would lead to the formation of the stable interface.

8 Conclusion

In this thesis we used O-theory with a 2 dimensional approach, in order to determine the interfacial match between to surfaces of two crystals. This allowed us determine the orientation in crystals in the plane of the interface boundary, and as a result we where able to find which other boundaries might arise as a result. This allowed us to identify which orientations would result in well matched interfaces, with little to no strain required to achieve the interface match and few grain boundary defects as result. By combining the insights from growth kinetics and databases of grain boundary energy densities, with the results from our model we where able to provide qualitative predictions on which conditions would allow for the formation of the desired interfacial match. Since the model is based on a purely geometric approach, decisively concluding whenever the formation of the desired interface match is possible is beyond the scope of the model. However, the model as presented here is highly useful under circumstances where we have an empirically founded idea of which out of plane orientations to expect.

8.1 Acknowledgments

I would like to express my sincerest gratitude to my supervisors Peter Krogstrup, and Tobias Særkjær, without whose guidance, patience, and insight, there would be no thesis.
Furthermore i would like to extend my gratitude to Thomas Kanne whose equally sagely guidance helped shaped the thesis into something presentable within the time frame set by the deadline.
Finally i want to express my thanks to my wonderful as-of-time-of-writing soon-to-be wife Kamille, and our lovely daughter Therese, while not providing any theoretical insights or discussion of subject matter of the this thesis, the thesis could not have been made without you by my side.

References

[1] *https://home.kpmg/dk/en/home/insights/2020/11/quantum-technology-could-be-denmark-s-next-business-adventure.html*

[2]] H. Kroemer *Rev. Mod. Phys. 73, 783 (2001)*

[3] Murthy, A. A., et al. *"TOF-SIMS analysis of decoherence sources in superconducting qubits." Applied Physics Letters 120.4 (2022): 044002.*

[4] A. Blom and K. Stokbro, *J. Comput. Electron. 12, 623 (2013).*

[5] W. Bollmann, *Crystal Defects and Crystalline Interfaces (Springer-Verlag Berlin Heidelberg, 1970)*

[6] P. Krogstrup, H. I. Jørgensen, E. Johnson, M. H. Madsen, C. B. Sørensen, A. F. i Morral, M. Aagesen, J. Nygård, and F. Glas (2013) *Advances in the theory of III–V nanowire growth dynamics.*

[7] T.Særkjær *Material Distributions and Equilibrium Faceting of SAG Structures*, 2020

[8] Matlab Code *https://sid.erda.dk/share_redirect/gFyE4nlcze*

Journal of Physics D: Applied Physics, 46(31), 313001.

[9] P. Krogstrup, N. L. B. Ziino, W. Chang, S. M. Albrecth, M. H. Madsen, E. Johnson, J. Nygård, C. M. Marcus, and T. S. Jespersen (2015) *Epitaxy of semiconductor–superconductor nanowires.*, Nature Materials, 14(4), 400–406.¨

[10] Zanolli Z, Fuchs F, Furthmüller J, von Barth U and Bechstedt F *2007 Phys. Rev. B 75 245121*

[11] *https://jp-minerals.org/vesta/en/download.html*

[12] Tran, Richard et al. (2017), *Data from: Surface energies of elemental crystals, Dryad, Dataset, https://doi.org/10.5061/dryad.f2n6f*

[13] Hui Zheng, Xiang-Guo Li, Richard Tran, Chi Chen, Matthew Horton, Donald Winston, Kristin Aslaug Persson, Shyue Ping Ong, *Grain boundary properties of elemental metals, Acta Materialia, Volume 186, 2020, Pages 40-49,ISSN 1359-6454, https://doi.org/10.1016/j.actamat.2019.12.030.*

[14] Kanne, T., Marnauza, M., Olsteins, D. et al. Epitaxial Pb on InAs nanowires for quantum devices. Nat. Nanotechnol. 16, 776–781 (2021). https://doi.org/10.1038/s41565-021-00900-9 *Epitaxial Pb on InAs nanowires for quantum devices. Nat. Nanotechnol. 16, 776–781 (2021)*

[15] Jelver, L., Larsen, P. M., Stradi, D., Stokbro, K., Jacobsen, K. W. (2017). *Determination of low-strain interfaces via geometric matching. Physical Review B, 96(8), [085306]. https://doi.org/10.1103/PhysRevB.96.085306*